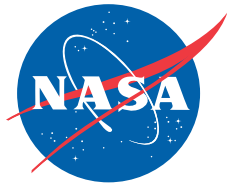


NASA/TM-2009-214648



Implementation of an Adaptive Controller System from Concept to Flight Test

*Richard R. Larson, John J. Burken, and Bradley S. Butler
NASA Dryden Flight Research Center
Edwards, California*

*Steve Yokum
West Virginia High Technology Consortium Foundation
Fairmont, West Virginia*

July 2009

NASA STI Program ... in Profile

Since its founding, NASA has been dedicated to the advancement of aeronautics and space science. The NASA scientific and technical information (STI) program plays a key part in helping NASA maintain this important role.

The NASA STI program operates under the auspices of the Agency Chief Information Officer. It collects, organizes, provides for archiving, and disseminates NASA's STI. The NASA STI program provides access to the NASA Aeronautics and Space Database and its public interface, the NASA Technical Report Server, thus providing one of the largest collections of aeronautical and space science STI in the world. Results are published in both non-NASA channels and by NASA in the NASA STI Report Series, which includes the following report types:

- **TECHNICAL PUBLICATION.** Reports of completed research or a major significant phase of research that present the results of NASA Programs and include extensive data or theoretical analysis. Includes compilations of significant scientific and technical data and information deemed to be of continuing reference value. NASA counterpart of peer-reviewed formal professional papers but has less stringent limitations on manuscript length and extent of graphic presentations.
- **TECHNICAL MEMORANDUM.** Scientific and technical findings that are preliminary or of specialized interest, e.g., quick release reports, working papers, and bibliographies that contain minimal annotation. Does not contain extensive analysis.
- **CONTRACTOR REPORT.** Scientific and technical findings by NASA-sponsored contractors and grantees.

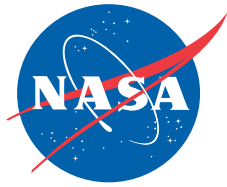
- **CONFERENCE PUBLICATION.** Collected papers from scientific and technical conferences, symposia, seminars, or other meetings sponsored or co-sponsored by NASA.
- **SPECIAL PUBLICATION.** Scientific, technical, or historical information from NASA programs, projects, and missions, often concerned with subjects having substantial public interest.
- **TECHNICAL TRANSLATION.** English-language translations of foreign scientific and technical material pertinent to NASA's mission.

Specialized services also include creating custom thesauri, building customized databases, and organizing and publishing research results.

For more information about the NASA STI program, see the following:

- Access the NASA STI program home page at <http://www.sti.nasa.gov>
- E-mail your question via the Internet to help@sti.nasa.gov
- Fax your question to the NASA STI Help Desk at 443-757-5803
- Phone the NASA STI Help Desk at 443-757-5802
- Write to:
NASA STI Help Desk
NASA Center for AeroSpace Information
7115 Standard Drive
Hanover, MD 21076-1320

NASA/TM-2009-214648



Implementation of an Adaptive Controller System from Concept to Flight Test

*Richard R. Larson, John J. Burken, and Bradley S. Butler
NASA Dryden Flight Research Center
Edwards, California*

*Steve Yokum
West Virginia High Technology Consortium Foundation
Fairmont, West Virginia*

*National Aeronautics and
Space Administration*

*Dryden Flight Research Center
Edwards, California 93523-0273*

July 2009

NOTICE

Use of trade names or names of manufacturers in this document does not constitute an official endorsement of such products or manufacturers, either expressed or implied, by the National Aeronautics and Space Administration.

Available from:

NASA Center for AeroSpace Information
7115 Standard Drive
Hanover, MD 21076-1320
(443) 757-5802

ABSTRACT

The National Aeronautics and Space Administration Dryden Flight Research Center (Edwards, California) is conducting ongoing flight research using adaptive controller algorithms. A highly modified McDonnell-Douglas NF-15B airplane called the F-15 Intelligent Flight Control System (IFCS) is used to test and develop these algorithms. Modifications to this airplane include adding canards and changing the flight control systems to interface a single-string research controller processor for neural network algorithms. Research goals include demonstration of revolutionary control approaches that can efficiently optimize aircraft performance in both normal and failure conditions and advancement of neural-network-based flight control technology for new aerospace system designs.

This report presents an overview of the processes utilized to develop adaptive controller algorithms during a flight-test program, including a description of initial adaptive controller concepts and a discussion of modeling formulation and performance testing. Design finalization led to integration with the system interfaces, verification of the software, validation of the hardware to the requirements, design of failure detection, development of safety limiters to minimize the effect of erroneous neural network commands, and creation of flight test control room displays to maximize human situational awareness; these are also discussed.

NOMENCLATURE

ail	aileron
alphad	angle of attack, deg
ang	normal acceleration, g
A	aircraft stability derivatives
AIU	avionics interface unit
AMUX	analog multiplexer
API	application program interface
ARTS	Airborne Research Test System
betad	angle of sideslip, deg
B	aircraft control derivatives
B_a	basis function
can	canard
C	neural network input category
CAT	Choose-a-Test
CC	central computer
CIU	cockpit interface unit
DAG	Dial-a-Gain
DFRC	Dryden Flight Research Center
DLL	design limit load
DR	discrepancy report
FC	flight computer
FCC	flight control computer
g	acceleration of gravity
Gen2_p_ad	Generation 2 roll adaptive command
Gen2_q_ad	Generation 2 pitch adaptive command
Gen2_r_ad	Generation 2 yaw adaptive command
G	adaptation gain

HWCI	hardware configuration item
iadadag	ada source of Dial-a-Gain
iadapal	ada source of Pick-a-Limit
IADS	Interactive Analysis and Display System
IFCS	Intelligent Flight Control System
I/O	input/output
kron	nested Kronecker product
K_d	derivative gain
K_i	integral gains
K_p	proportional gain
K_z	learning gains
K_{z_i}	learning gains integral
L	error-modification term
MCC	Mission Control Center
MPD	multi-purpose display
MPDP	multi-purpose display processor
MUX	multiplex
NASA	National Aeronautics and Space Administration
NN	neural network
NVRAM	non-volatile random access memory
N_y	y-axis normal load factor
N_z	z-axis normal load factor
OFP	operational flight program
p	roll rate, deg/s
pbodyd	roll rate body axis, deg/s
phi	roll angle
phid	roll angle, deg
p-i-d	proportional-integral-derivative
PAL	Pick-a-Limit
PC	personal computer
PID	parameter identification
PLA	power level angle
PTC	portable test computer
PVI	pilot-vehicle interface
q	pitch rate, deg/s
qbodyd	pitch rate body axis, deg/s
r	yaw rate, deg/s
rbodyd	yaw rate body axis, deg/s
rud	rudder
stab	stabilator
SES	simulation electric stick
SW	software
thetad	pitch angle, deg
U_{ad}	augmentation command
U_{dd}	error compensation commands
u	surface positions
u_c	surface deflections commands
V&V	verification and validation

W	neural network weights
\dot{W}	neural network weight derivative
W^T	neural network weight transpose
x	aircraft state
\dot{x}	aircraft state derivative
x_e	aircraft state error
\dot{x}_e	aircraft state derivative command
x_{ref}	angular body axis rate
\dot{x}_{ref}	angular body axis acceleration
Z	neural network learning signal

INTRODUCTION

There is interest in investigating possible future technologies by performing flight-test research using neural network (NN) adaptive controllers. The use of NN and similar adaptive technologies in the design of highly fault- and damage-tolerant flight control systems shows promise toward increasing the survivability of future aircraft by maintaining the integrity of the flying qualities of the aircraft as much as possible in the presence of certain failures. Addressing this challenge, the National Aeronautics and Space Administration Dryden Flight Research Center (DFRC) at Edwards Air Force Base (AFB) (Edwards, California) formed the F-15 Intelligent Flight Control System (IFCS) program, which uses a highly modified McDonnell-Douglas NF-15B test airplane (tail number 837) to conduct research. The F-15 IFCS airplane, shown in fig. 1, incorporates a quadruplex all-digital flight control system that interfaces with the NN processor; the addition of canards; and thrust-vectoring nozzles.

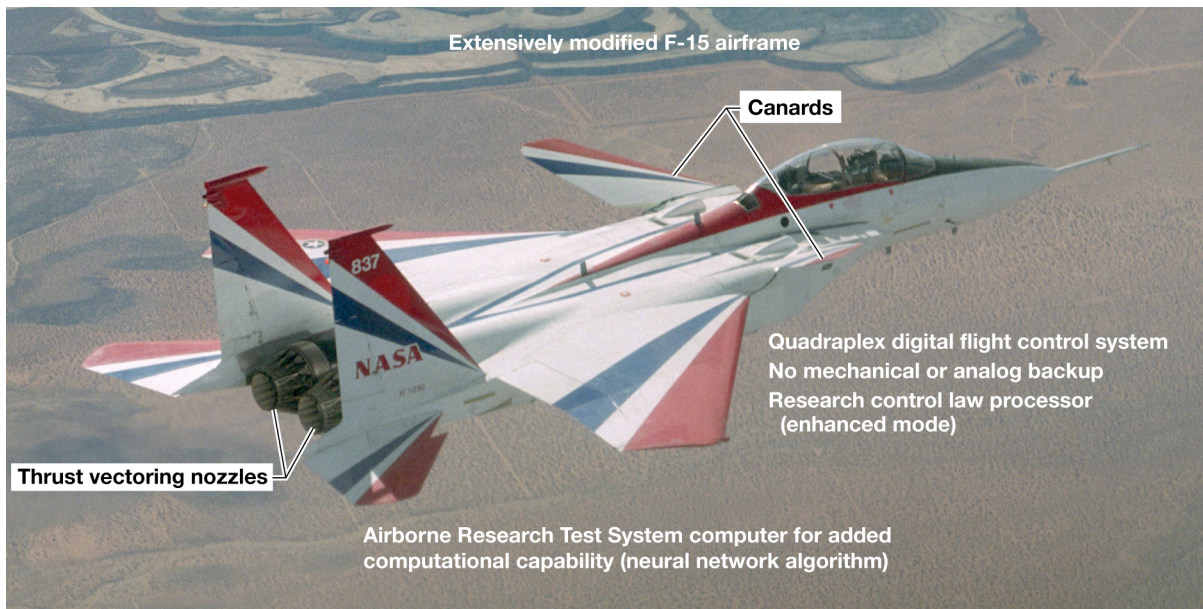


Figure 1. The F-15 Intelligent Flight Control System airplane, tail number 837.

Early in the F-15 IFCS program, a design decision was made to interface the NN controller in a single processor with the existing flight control computers (FCCs). This single-string approach rendered the software and hardware less complicated, but added risk due to lack of redundancy. This report presents the processes used to develop adaptive controller algorithms throughout the progression of a flight-test program. Many challenges existed toward making this research cost-effective, timely, efficient, and, most importantly, safe; an overview of the tasks related to these challenges is presented. Some of the approaches discussed herein may be applied to future flight-test activities.

SIMULINK[®] ALGORITHMS

The NN adaptive flight control system architecture, shown in figure 2, is based on the augmented model inversion controller developed by Calise, Lee, and Sharma (ref. 1), and Rysdyk and Calise (ref. 2). An explicit model-following scheme is used to achieve the desired handling qualities. This direct adaptive approach integrates feedback linearization theory with on-line learning sigma-pi NNs. These networks generate command augmentation signals to compensate for errors in the model inversion. A Lyapunov stability proof guarantees boundedness of the tracking error and network weights.

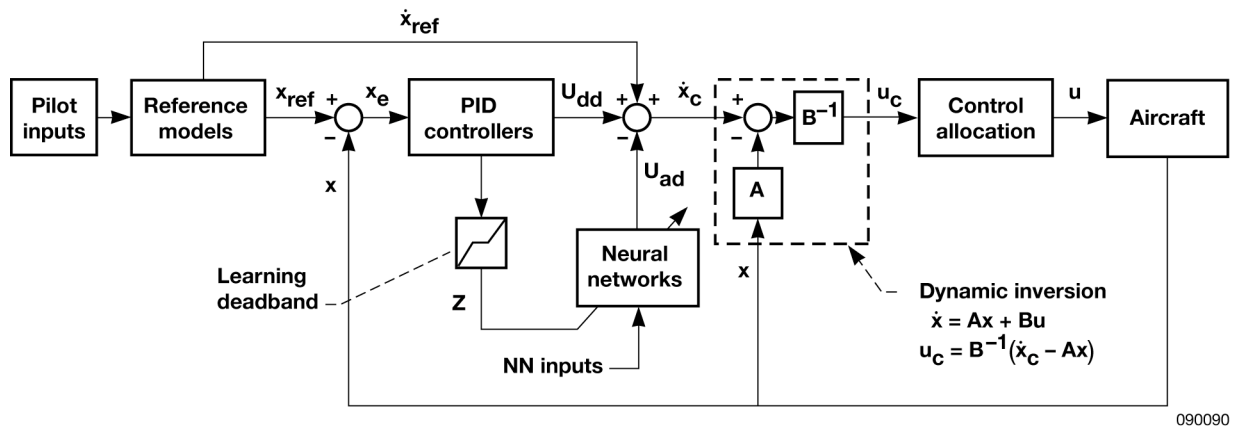


Figure 2. The neural adaptive flight control system architecture.

The pilot generates flight commands through longitudinal and lateral stick deflections and use of the rudder pedals. The flight commands are then filtered through reference models that produce angular body axis rate (x_{ref}) and angular body axis acceleration (\dot{x}_{ref}) signals with the desired frequency and damping characteristics (ref. 3). Dynamic inversion is then used to compute the necessary surface deflections commands (u_c) to achieve the desired accelerations. If the dynamic inversion and aircraft dynamics behaved together as a perfect integrator, then the response of the aircraft would match the reference models. Since errors are introduced by inaccuracies in the inversion, however, proportional-integral-derivative (p-i-d) controllers are necessary to generate error compensation commands (U_{dd}), as shown in equation (1) below,

$$U_{dd} = K_i \int x_e + K_p x_e + K_d \dot{x}_e \quad (1)$$

where x_e is the state error, K_p is the proportional gain, and K_d is the derivative gain.

The NNs work in conjunction with the p-i-d controllers by recognizing error patterns and learning how to compensate for them through the generation of augmentation commands (U_{ad}). The selected NN inputs consist of sensor feedback (for A -matrix failures), control commands (for B -matrix failures), and bias terms (for out-of-trim conditions). These inputs are normally separated into different neural network input categories (C), which are then combined together to form a basis function (B_a) using nested Kronecker products, as shown in equation (2) below.

$$B_a = \text{kron}(\text{kron}(C_1, C_2), C_3) \dots \quad (2)$$

This basis function can then be used to update the neural network weights (W) with an adaptation law, as shown in equation (3) below, and to compute the augmentation command (U_{ad}), as shown in equation (4) below.

$$\dot{W} = -G(ZB_a + L|Z|W) \quad (3)$$

$$U_{ad} = W^T B_a \quad (4)$$

The adaptation gain (G) specifies how fast the weights will adapt. The error-modification term (L) helps to contain the growth of the weights. The neural network learning signal (Z) is computed as a function of error, as shown in equation (5) below, with learning gains (K_z) that are conditionally based upon the dynamic inversion p-i-d controller gains. In equation (5), the subscripts p and d refer to proportional and derivative, respectively.

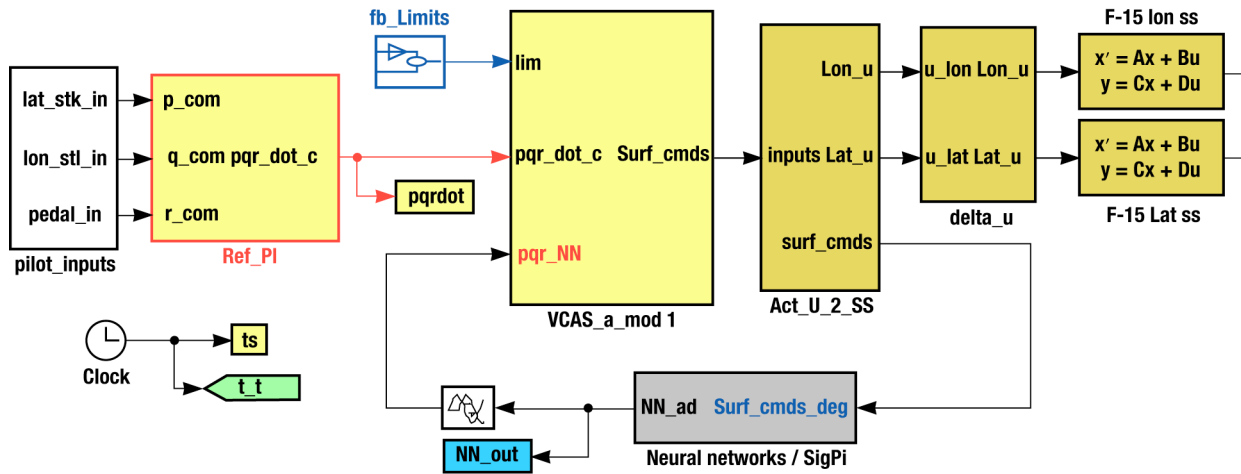
$$Z = K_{z_i} \int x_e + K_{z_p} x_e + K_{z_d} \dot{x}_e \quad (5)$$

The role of dynamic inversion is provided by a pseudo-inverting Versatile Control Augmentation System (VCAS), developed by the Boeing Phantom Works at Saint Louis, Missouri (The Boeing Company, Chicago, Illinois). The objectives of this improved adaptive controller algorithm, Generation 2a, called Gen 2a, will now be discussed.

Generation 2a Enhancements

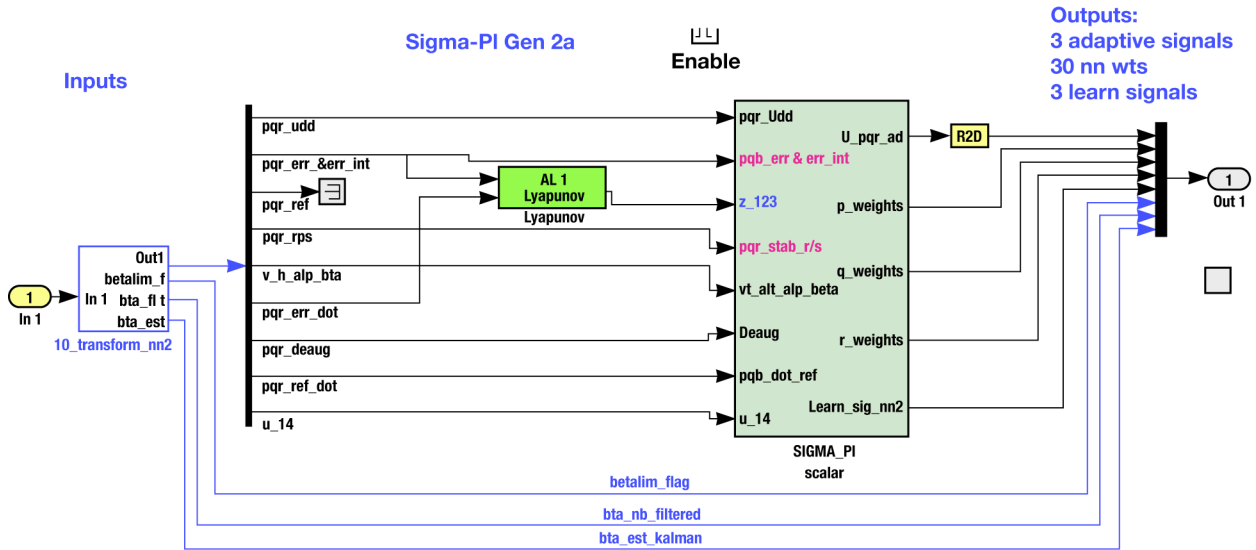
The performance objectives of the F-15 NN adaptive flight control tests include restoring model-following tracking performance, reducing cross-coupling effects, and reducing initial transients caused by failure insertion. For piloted aircraft applications, the NNs must adapt quickly enough to assist pilots in controlling a damaged aircraft, yet avoid learning transients that could interfere with the pilot's ability to control the aircraft during adaptation. The Gen 2a enhancements improved the performance of the adaptive system (ref. 4). The design team processed equations (1) through (5) into MATLAB[®] and Simulink[®] (both registered trademarks of The MathWorks, Inc., Natick, Massachusetts) block diagrams. Figure 3 shows the top level of the flight control system with NNs that were processed by Simulink[®] AutoCode into the C computer language.

From figure 3, the block diagram is broken down into a smaller Simulink[®] AutoCode subsystem shown in figure 4. At this time the Simulink[®] AutoCode is generated which is used in the six-degrees-of-freedom simulation and eventually in the aircraft FCC in the form of an operational flight program (OFP). The OFP is the final step after many tests have been performed in the six-degrees-of-freedom simulation, including pilot-in-the-loop testing.



090091

Figure 3. The top level of the flight control system with neural networks.



090092

Figure 4. The Simulink® AutoCode block diagram.

AIRBORNE RESEARCH TEST SYSTEM SOFTWARE DEVELOPMENT

The airborne research test system (ARTS) is a flight-ruggedized processor system dedicated to the execution of flight research software, in this case NN adaptive control. The ARTS was developed by the West Virginia High Technology Consortium (WVHTC) Foundation (Fairmont, West Virginia) in support of the IFCS. The architecture is a system of three single-board computers with a variety of input/output (I/O) options to support a large set of potential research initiatives. Each computer is a 400 Mhz PowerPC with 256 MB of RAM. Two of the computers are dedicated to the execution of research, and one computer handles the system interfaces. Inter-board communication is performed using the VME backplane. All single-board computers run the VxWorks® (Wind River Systems, Inc., Alameda, California) real-time operating system.

The baseline ARTS software load has no pre-knowledge of the research algorithms that it will be executing. An executive framework is in place to handle the communication with the aircraft data buses, and an application program interface (API) mechanism allows research experiments to register their existence and communicate, via the I/O computer, with the aircraft flight controls. This architecture keeps the ARTS generic while providing an interface to the aircraft for the research experiments.

Research flown on the ARTS to date has been developed using the MathWorks Simulink[®] software development environment. The process of integrating the Simulink[®] model into the ARTS involves Simulink[®] AutoCoding the model to the C computer language and later importing to a PowerPC. The Simulink[®] model conversion process is shown in figure 5. A wrapper of C-language hand code is then written around the I/O of the model to receive and forward the aircraft state data to the Simulink[®] AutoCoded model as well as to transmit command augmentations from the model back to the aircraft flight controls. This transfer of information is achieved using the APIs provided by the flight executive. Additionally, APIs are provided to record any required state data of the model to non-volatile random access memory (NVRAM) solid-state disk drives within the ARTS. These disk drives may be retrieved post-flight for additional analysis.

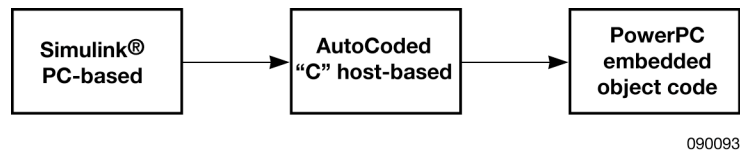


Figure 5. The Simulink[®] model conversion process.

Validating proper integration of the Simulink[®] model is a three-phase process. The developer of the model provides a check-case with a set of inputs and a set of expected outputs. That check-case is first executed within the native Simulink[®] environment to validate that it matches on the machine that will perform the Simulink[®] AutoCoding. The Simulink[®] model is then Simulink[®] AutoCoded to the C language. The C code and the check-case are then executed again on a host processor (typically a UNIX derivative) to validate that the check-case still matches. The check-case validation architecture is shown in figure 6. Once confidence in the C code is established, the code is compiled for VxWorks[®] and integrated with the ARTS APIs. The check-case is then executed using a hardware-in-the-loop simulation (HILS). This HILS is executed on a PC with 1553 I/O capabilities that simulate the 1553 buses on the aircraft. The results of the check-case are compared against the original for an acceptable tolerance. The check-case will never match exactly due to the fact that 64-bit floating point signals are scaled to 16 bits for insertion on the 1553 bus.

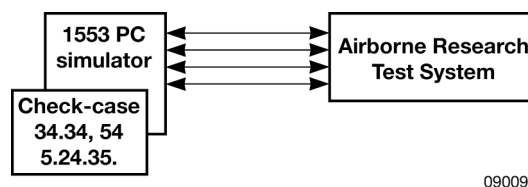


Figure 6. The check-case validation architecture.

AIRBORNE RESEARCH TEST SYSTEM DESIGN

The ARTS architecture showing its interface with the F-15 IFCS is shown in figure 7. The ARTS is a remote terminal (RT) to the FCC and the central computer (CC). It is a bus controller to the instrumentation systems and also features an analog multiplexer (AMUX) card to interface with analog signals. The NN experiment options are controlled by the pilot using the existing multi-purpose display (MPD) panel in the cockpit. This display panel allows a pilot-vehicle interface (PVI) with the ARTS. The NN algorithm engagement options, along with variable gain sets for each function, can be controlled by the pilot. The gain sets are used to alter the states within the model and provide a means to configure the software without a necessitating a recompile.

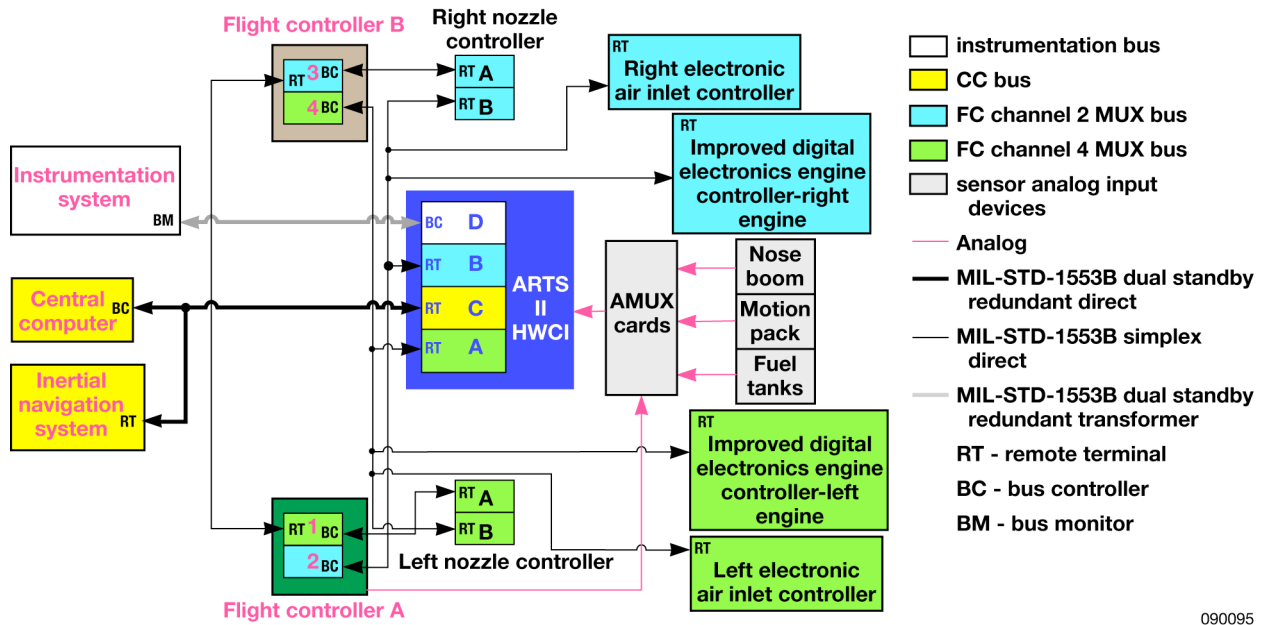


Figure 7. The F-15 Intelligent Flight Control System architecture.

Pilot-Vehicle Interface

Three functions are used to select the experiment configuration and options: Pick-a-Limit (PAL); Dial-a-Gain (DAG); and Choose-a-Test (CAT). An image of the MPD showing these options is presented in figure 8.

The PAL is used to define the flight limits. There are two possible flight envelope ranges, depending on the PAL number selected, as shown in table 1. If any of the parameters shown in table 1 are outside of the flight envelope range, the system will downmode to the conventional flight control laws. A unique downmode flag is set on the 1553 bus and monitored in the mission control center (MCC).

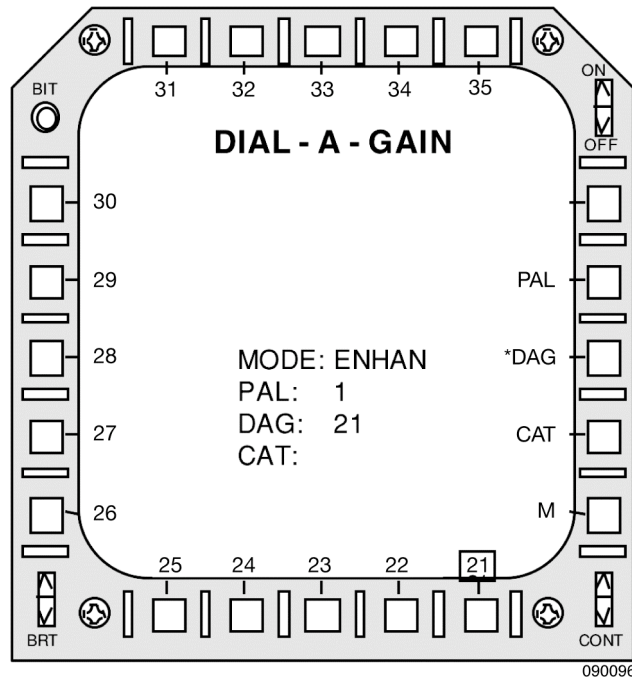


Figure 8. The multi-purpose display Intelligent Flight Control System functions.

Table 1. Pick-a-Limit flight envelope limits.

Parameter	Envelope #1 (PAL 0-7)		Envelope #2 (PAL 8-15)	
	Lower limit	Upper limit	Lower limit	Upper limit
Angle of attack	-4.0 deg	12.0 deg	-4.0 deg	12.0 deg
Sideslip angle	-5 deg	5 deg	-5 deg	5 deg
Pitch angle	-180 deg	180 deg	-180 deg	180 deg
Bank angle	-90 deg	90 deg	-180 deg	180 deg
Pitch rate	-45 deg/sec	45 deg/sec	-60 deg/sec	60 deg/sec
Roll rate	-75 deg/sec	75 deg/sec	-300 deg/sec	300 deg/sec
Yaw rate	-15 deg/sec	15 deg/sec	-60 deg/sec	60 deg/sec
Normal acceleration [1]	-1 g	2.1 g	-2.0 g	5.0 g
Lateral acceleration	-0.5 g	0.5 g	-1.0 g	1.0 g
Mach number	0.55	0.95	0.55	0.95
Qbar	253 psf	733 or 550 psf ²	253 psf	733 or 550 psf ²
Altitude	15,000 ft	35,000 ft	15,000 ft	35,000 ft
Pitch stick	-3.1 in	5.46 in	-3.1 in	5.46 in
Roll stick	-4.0 in	4.0 in	-4.0 in	4.0 in
Yaw pedal	-3.25 in	3.25 in	-3.25 in	3.25 in
Throttle (PLA)	16.5 deg	130 deg	16.5 deg	130 deg
Discrete switches				PAL 15 only
Flap up mode	1 U		1 U	2 DM
Landing gear up	2 DM		2 DM	0 LGD
Throttle switch up	2 DM		2 DM	2 DM
Spin mode	0 NS		0 NS	0 NS
Weight on wheels	0 NGC		0 NGC	1 GC

Legend for discrete switches: DM = doesn't matter; GC = ground contact; LGD = landing gear down; NGC = no ground contact; NS = no spin; U = up.

For every PAL selected there is a DAG option which can be engaged to either create a particular type of failure in the FCC (a stabilator lock or a canard gain multiplier) or a surface excitation signal for parameter identification (PID) testing. There are eight DAG sets, one of which is shown in table 2. In this example, various stabilator lock values or canard multiplier failures may be set by the FCC. An excitation signal may also be activated after a failure is set, or the excitation signal can be commanded independently.

Table 2. Dial-a-Gain options.

PAL	DAG	Flying qualities	Failure	Excitation	Qbar limit
1 or 8	20	Baseline	None	None	733 psf
	21	Baseline	4 deg left stabilator lock	None	550 psf
	22	Baseline	2 deg left stabilator lock	None	733 psf
	23	Baseline	0 deg left stabilator lock	None	733 psf
	24	Baseline	-2 deg left stabilator lock	None	733 psf
	25	Baseline	-4 deg left stabilator lock	None	550 psf
	26	Baseline	-0.5 canard failure multiplier	None	550 psf
	27	Baseline	-0.2 canard failure multiplier	None	733 psf
	28	Baseline	0 canard failure multiplier	None	733 psf
	29	Baseline	0.1 canard failure multiplier	None	733 psf
	30	Baseline	0.2 canard failure multiplier	None	733 psf
	31	Baseline	0.4 canard failure multiplier	None	733 psf
	32	Baseline	0.6 canard failure multiplier	None	733 psf
	33	Baseline	0.8 canard failure multiplier	None	733 psf
	34	Baseline	None	None	733 psf
	35	Baseline	None	None	733 psf

The CAT page is used to engage a particular NN for flight-testing, as shown in table 3. There were three NNs available in the ARTS OFP with possible beta sources as an input to the NN. The option to select multiple beta sources was added to the NN gain set files because of the uncertainty of the quality of the beta signal. This design allowed for particular configuration changes to be made without having to create and compile a new OFP. These configuration files, called CONFIG files, included unique options within the NN for each CAT.

Table 3. Choose-a-Test options.

CAT #	Neural network type	Beta source
40	None	
41	NN1 sigma Pi baseline	N/A
42	NN1 sigma Pi option 1	N/A
43	NN1 sigma Pi option 2	N/A
44	NN1 sigma Pi option 3	N/A
45	NN1 sigma Pi option 4	N/A
46	NN2 scalar baseline	Nose boom beta
47	NN2 scalar option 1	Filtered nose boom beta
48	NN2 scalar option 2	CC beta
49	NN2 scalar option 3	Estimated beta
50	NN3 scalar baseline	Nose boom beta
51	NN3 scalar option 1	Filtered nose boom beta
52	NN3 scalar option 2	CC beta
53	NN3 scalar option 3	Estimated beta
54	None	
55	None	

Configuration Files

The CONFIG files for the NNs included options to modify various parameters such as gains, limits, deadzones for each feedback signal, upper and lower weight limits, surface limits, and flags. A software tool was developed to ftp the existing configuration files from the ARTS OFP, replace the files that had been modified, recompute the checksums, and create a new zipped TAR file for import to the ARTS OFP.

Non-volatile Random Access Memory

The ARTS OFP provided for a set of NN signals to be written to NVRAM within the processor. Each time the NN was engaged, a predefined data set began writing to the NVRAM and continued until the NN was disengaged. The data file was retrieved from the ARTS after the flight using a portable test computer (PTC) that interfaced with the ARTS using an Ethernet connection.

Log Files

In addition to the NVRAM files the ARTS wrote log files, which provided status information such as modes transitions, errors, and file opening or closing status. The log file was retrieved after each flight and was particularly useful for troubleshooting. An excerpt from a log file is shown immediately below. The log file segment shown has flagged transition events within the ARTS of an NN engagement (CAT 51).

01:29:14, 321483, Severity:SUCCESS, Task:exec, Procedure:state_change.c, Details:Exec transitioned from the DISENGAGED to the ENGAGED state because FC requested Engagement

01:29:52, 323816, Severity:INFORMATIONAL, Task:exec, Procedure:process_cats.c, Details:CAT value of 51 coupled

01:29:58, 324169, Severity:INFORMATIONAL, Task:exec, Procedure:mode.c, Details:CAT mode changed from NOT_COUPLED to COUPLED

01:30:09, 324802, Severity:INFORMATIONAL, Task:exec, Procedure:mode.c, Details:CAT mode changed from COUPLED to CL_NN

FORMAL VERIFICATION AND VALIDATION TESTING

The verification and validation (V&V) of the new NN software release was performed in-house by NASA DFRC IFCS project personnel. An overview of the DFRC simulation architecture is shown in figure 9. The simulation featured a cockpit for piloted simulations with a projection screen for situational awareness, a full six degrees of freedom, hardware interfaces for the ARTS and the CC, and a functional MPD in the cockpit. A PTC was used to load and retrieve files in the ARTS. A PASS 3200 1553 bus analyzer was part of the PTC and was used for bus testing. All of the NN OFP V&V was performed with this system.

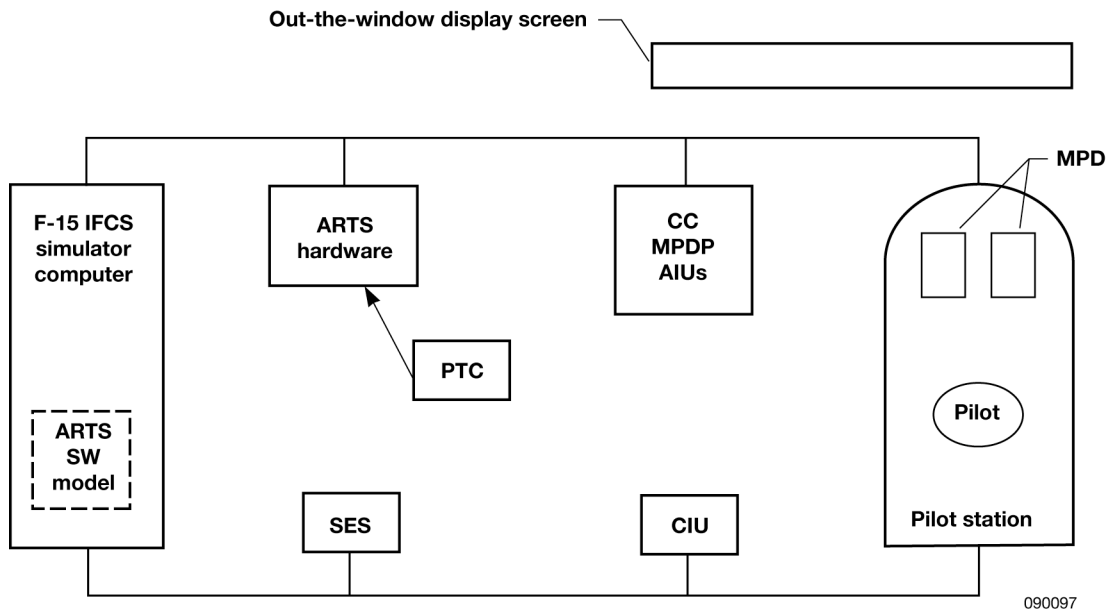
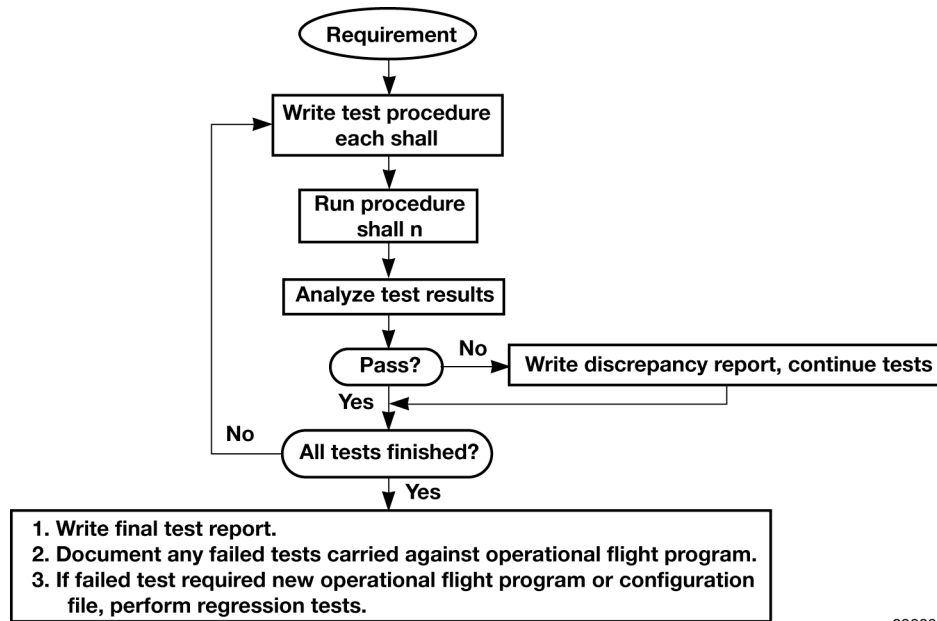


Figure 9. The F-15 Intelligent Flight Control System NASA Dryden simulation architecture.

The software V&V process is shown in figure 10. A formal V&V test plan was written, which included absolute requirements that are referred to as “shall statements.” Test procedures that contained simulation scripts for the test inputs and recorded output files were written for each requirement. This method produced more repeatability in the results and a faster, more automated execution of the procedures. All results referenced the test requirement “shall statement number.” A PASS or FAIL criteria was applied to the test results by both the test conductor and a witness. A test results document containing subsets of the recorded testing data was written. All failed tests were documented in

discrepancy reports (DRs). The DRs were categorized as a required fix, a minor limitation, or a procedure work-around. When a failed test was encountered, the tests continued to completion. The only exception was if the failed test was unacceptable and required a new OFP; for these tests there were no DRs in this category, however, there were DRs that were corrected at the conclusion of the V&V by using a new configuration file that did not require a new OFP. A selected subset of retests were performed for regression testing to complete the final V&V. Other discrepancies were found that would have required a new OFP, but these were considered minor, were consequently carried as DRs against the system, and were not fixed.



090098

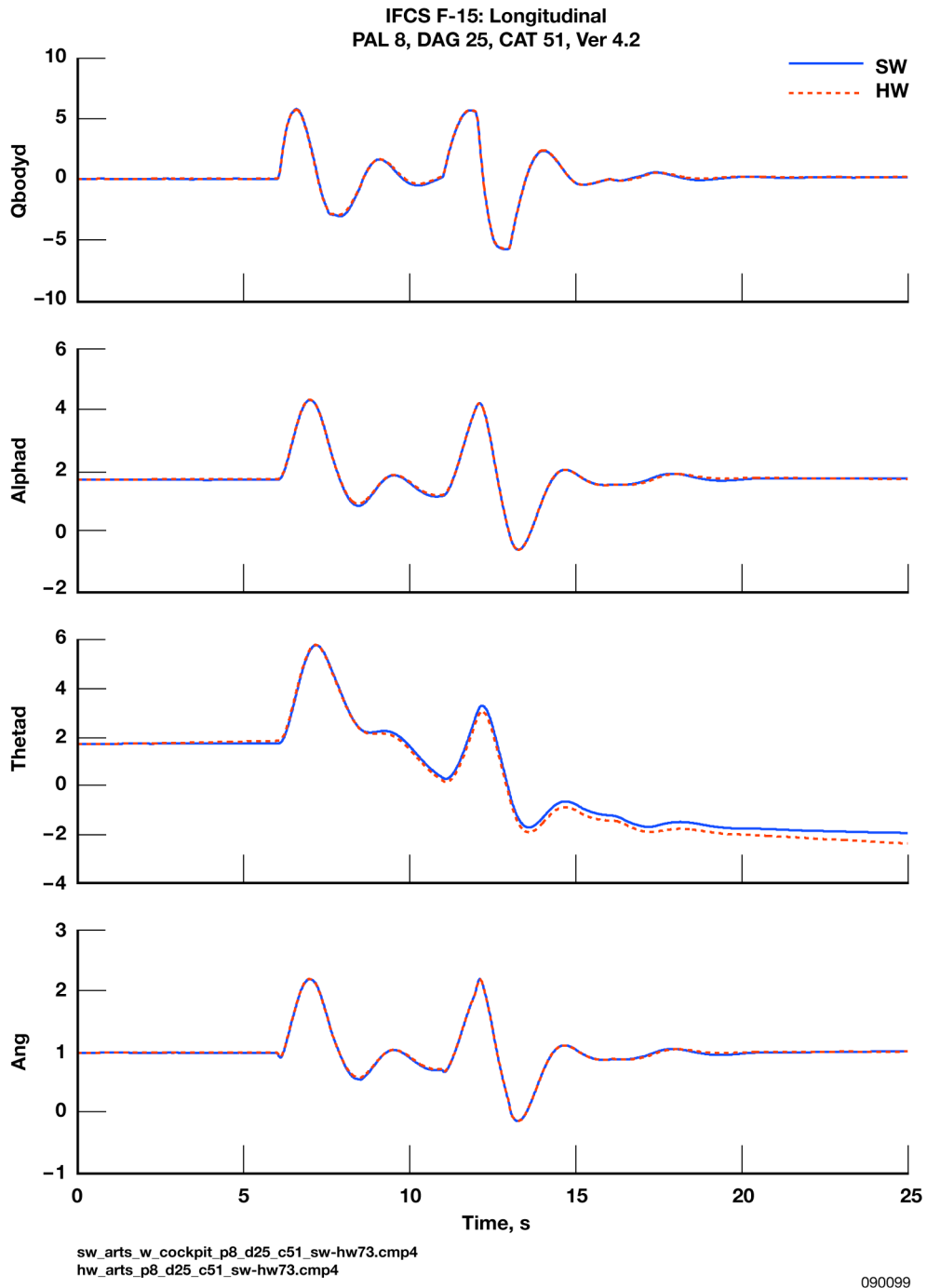
Figure 10. The software verification and validation process.

Verification and Validation Testers

Verification and validation tests were divided among the IFCS team according to the team members' area of expertise. The testing included: corrected DRs; new system requirements; comparisons of software versus hardware for no NN; NN(123) without failures; NN(123) with failures; 1553 bus testing; NVRAM; configuration files; piloted evaluations of the NN performance and NN disengagement transients; simulated structural loads; OFP path coverage; and failure modes and effects testing (FMET).

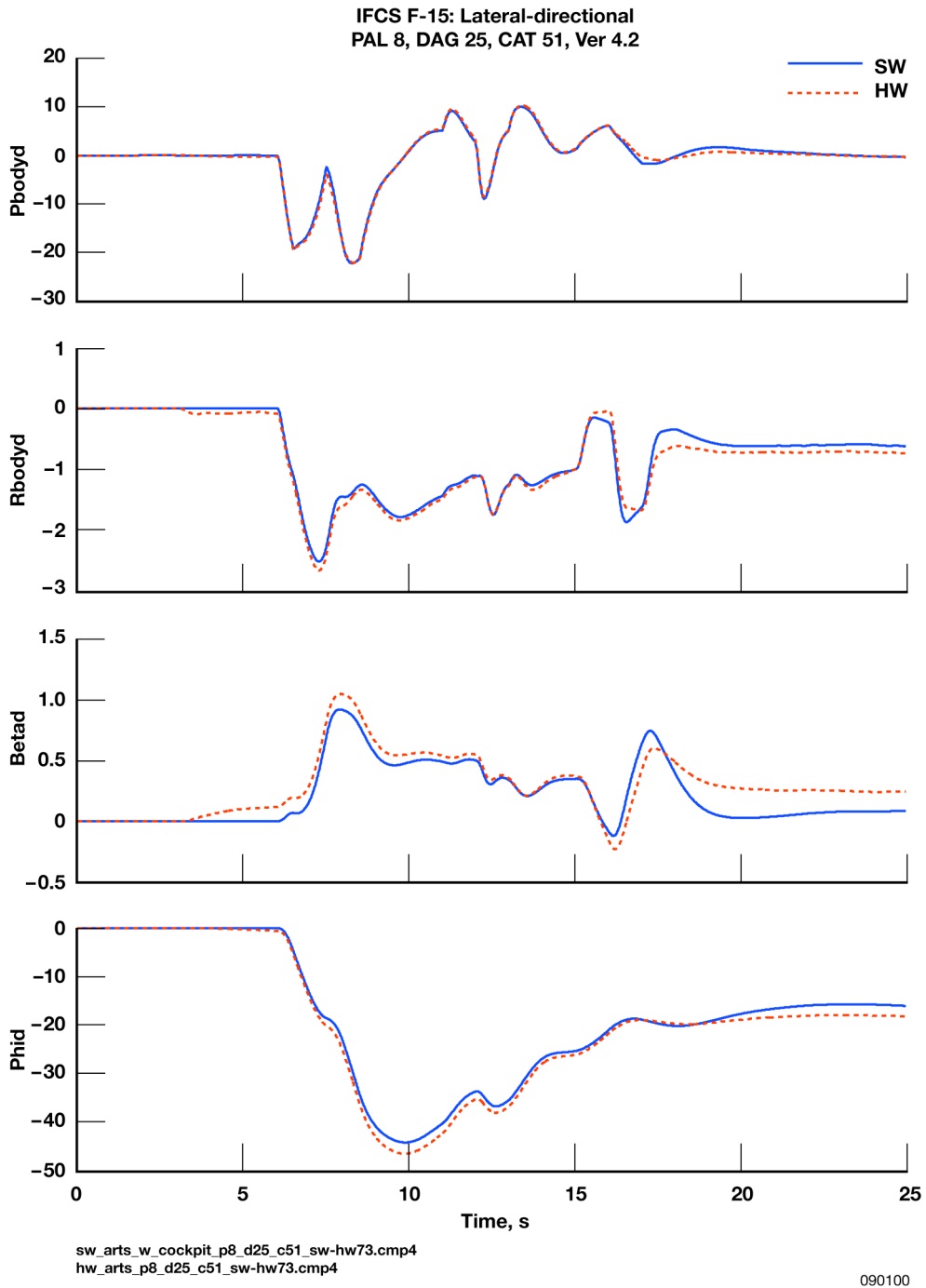
Sample Verification and Validation Test Results

Four sets of sample test verification test results are shown in figures 11(a) through 11(d). Attitudes, rates, and accelerations are shown in figures 11(a) and 11(b); surface positions comparisons are shown in figure 11(c); and NN commands are shown in figure 11(d). These time histories show the comparisons of the all-software version of the NN versus the NN interfaced with the simulation from the ARTS hardware. A simulation script was used to generate pitch, roll, and yaw stick and rudder pedal doublets.



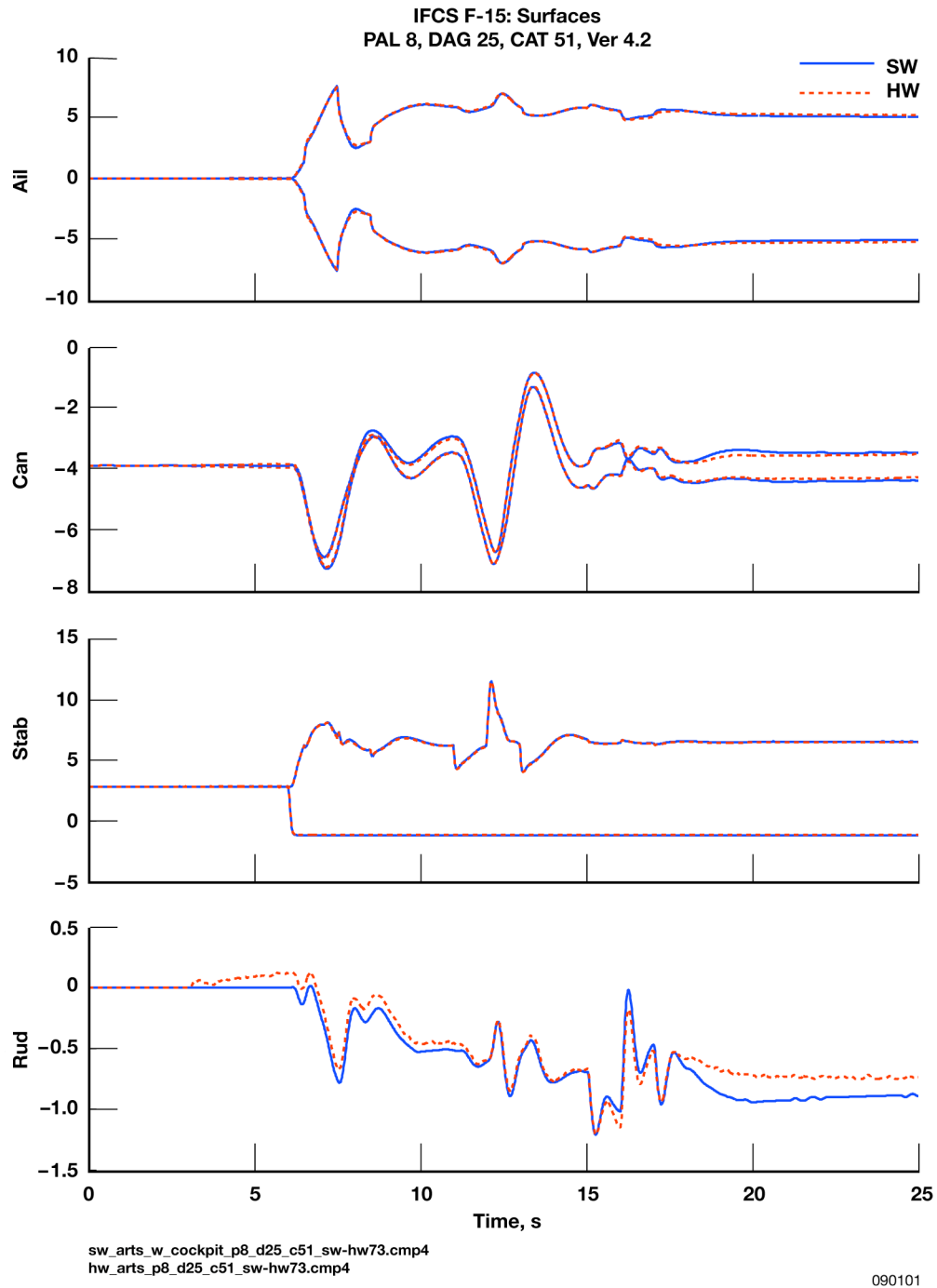
(a). Simulation comparisons of software versus hardware, Airborne Research Test System, set 1.

Figure 11. Simulation comparisons of software versus hardware, Airborne Research Test System, sets 1 through 4.



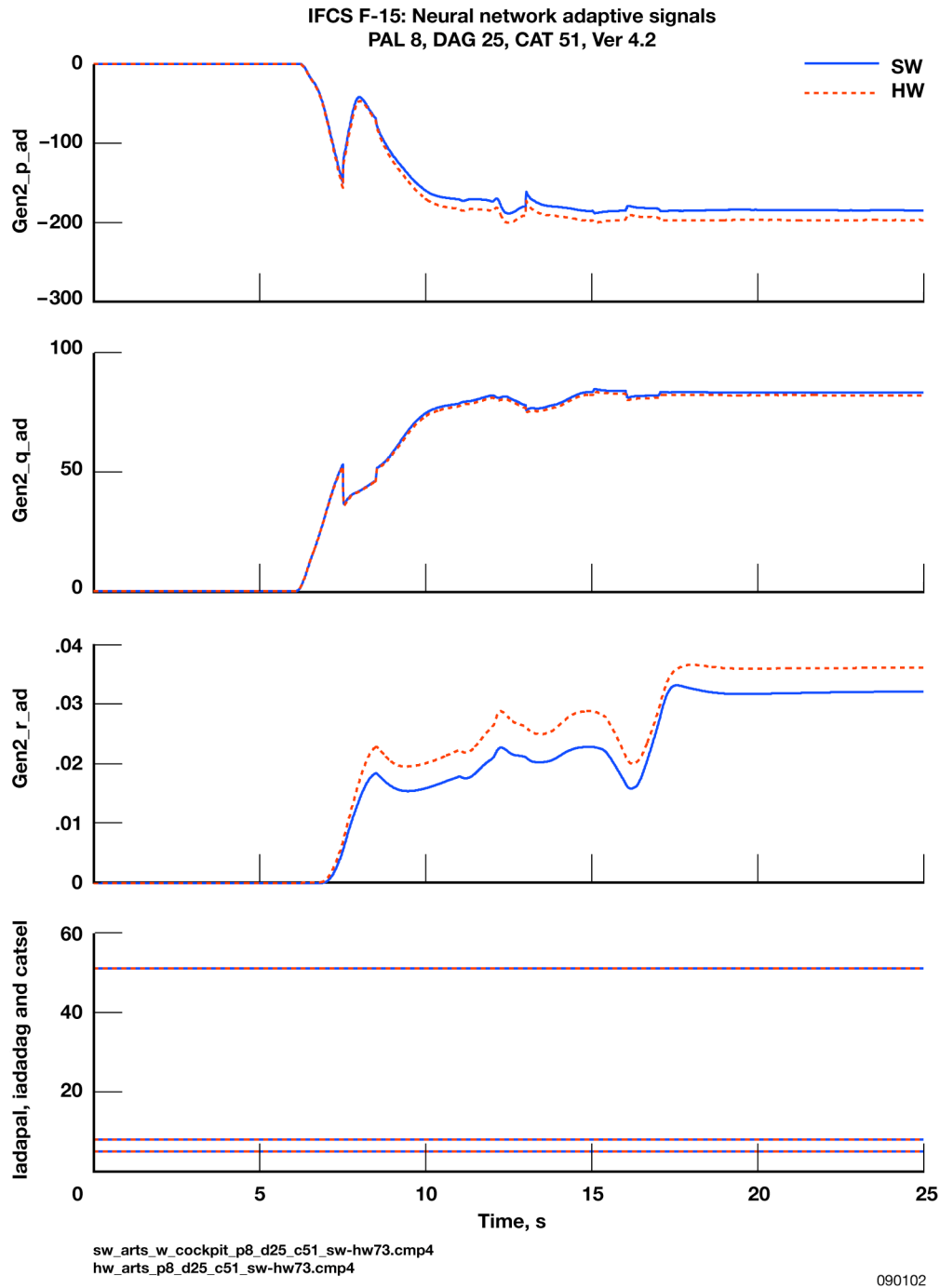
(b). Simulation comparisons of software versus hardware, Airborne Research Test System, set 2.

Figure 11. Continued.



(c). Simulation comparisons of software versus hardware, Airborne Research Test System, set 3.

Figure 11. Continued.



(d). Simulation comparisons of software versus hardware, Airborne Research Test System, set 4.

Figure 11. Concluded.

A sample of a piloted validation evaluation test card is shown in figure 12. This test was a handling qualities evaluation using one of the NN designs; the NN performed as expected. There were numerous test cards flown to evaluate each NN for nominal, with induced DAG-type failures, various piloted maneuvers and flight conditions, disengage transients, and system-type fault insertions. All of the results of these tests were determined to be acceptable.

TEST PURPOSE: VERIFY THAT THE GEN-2A ADAPTIVE SYSTEM EXHIBITS ACCEPTABLE HANDLING QUALITIES FOR THE OFF-NOMINAL FLIGHT CONDITION, NO FAILURES

TEST NOTES: THIS TEST WAS PERFORMED BY AN ENGINEERING PILOT.

REQUIREMENTS: 6.7.1-1.

TEST RESULTS: ALL PAL, DAG AND CAT SELECTIONS WORKED AS EXPECTED, AND THE AIRPLANE ENGAGED AND DISENGAGED PROPERLY. AT THE BOTH THE HIGH-QBAR AND LOW-QBAR TEST CONDITIONS, THE AIRCRAFT EXHIBITED GOOD FLYING CHARACTERISTICS FOR THETA CAPTURES, BANK-TO-BANK TURNS AND 3-G WINDUP TURNS.

ENGAGE TRANSIENTS LEVELS: NONE

DISENGAGE TRANSIENTS LEVELS: (NZ AND NY IN G'S, R IN DEG/SEC)

Maneuver	High Qbar			Low Qbar		
	nz	ny	r	nz	ny	r
theta captures	0.0	0.08	0.7	0.0	0.03	0.25
bank-to-bank turns	0.0	0.06	0.3	0.0	0.03	0.25
3-g wind-up turns	0.0	0.07	0.35	0.0	0.03	0.35

During the high- and low-qbar tests, yaw-axis weights #1, 3, 4 and 6 continued to grow throughout each test, producing a growing gen2_r_ad command. However, their values remained small (much less than one) and resulted in minor yaw rate disengage transients. 090103

Figure 12. A sample piloted evaluation flight card.

SAFETY MONITORS

The NN controller is a single-string interface to the FCC, therefore, the primary concern was that the worst-case failure would likely be an erroneous NN command hardover (rapid and sustained displacement of an aircraft aerodynamic control surface) to the FCC control laws. This type of command could result in excessive structural loads and g acceleration excursions to the aircraft. The pilot also imposed an additional requirement of no more than $\pm 0.5 g$ lateral and $\pm 2 g$ normal accelerations from trimmed flight for any disengagement transient. Safety monitors, which would disengage the NN and revert to the conventional control laws for most failures, were added in the FCC processors. These safety monitors will now be described.

Pick-a-Limit Monitor

The PAL monitor generates a downmode from the NN when any limit is exceeded, as was briefly described in the “Pilot-Vehicle Interface” section above. If any limit was exceeded, the IFCS would revert to the conventional control system. This monitor, however, did not prevent the g limits from being exceeded for a NN hardover. A graphical representation of this problem is shown in figure 13. An NN hardover was inserted in the pitch-up direction, causing the PAL limiter to trigger a disengagement at $6 g$, but due to the momentum of the aircraft, the response peaked at approximately $10.5 g$. A similar result for the roll axis is shown in figure 14. In this case, the PAL safety monitor was never set because the lateral acceleration never reached the limit. These responses are both unacceptable, thus, a new monitor, called a floating limiter, was developed and added to the FCC software. The floating limiter proved to be a much better concept for controlling both the structural loads and g excursions. As shown in figures 13 and 14, this new monitor limited the g excursion to approximately $2.3 g$, which was far more effective in producing the desired results.

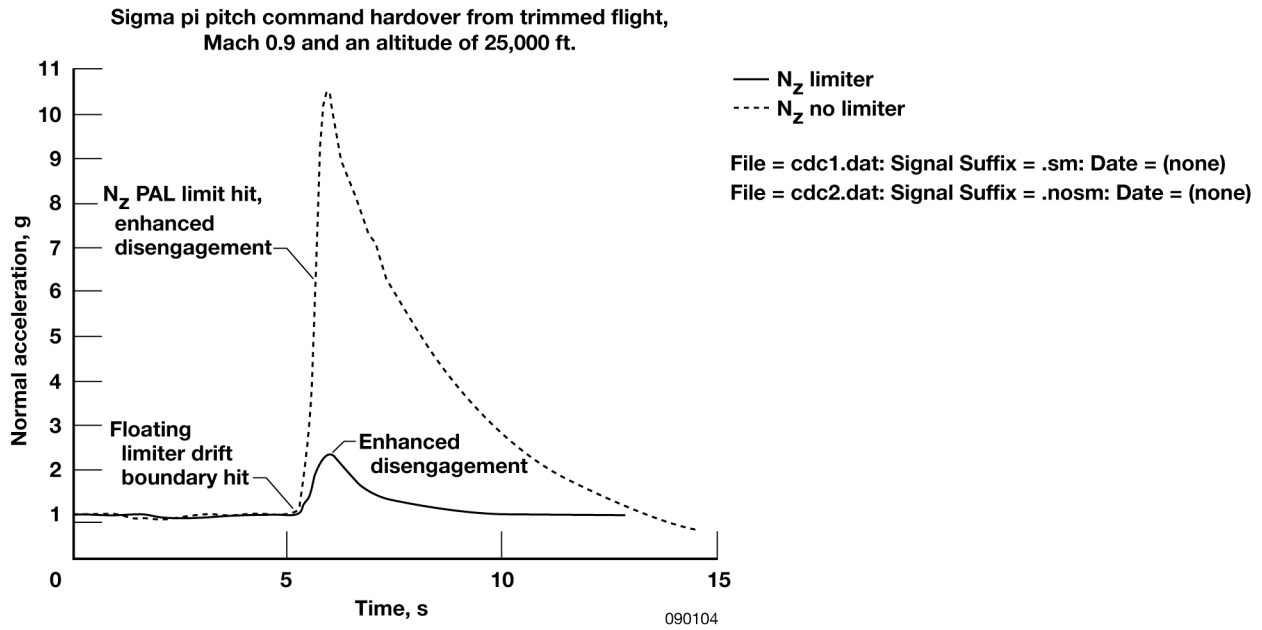


Figure 13. Normal acceleration response due to an Airborne Research Test System pitch hardover.

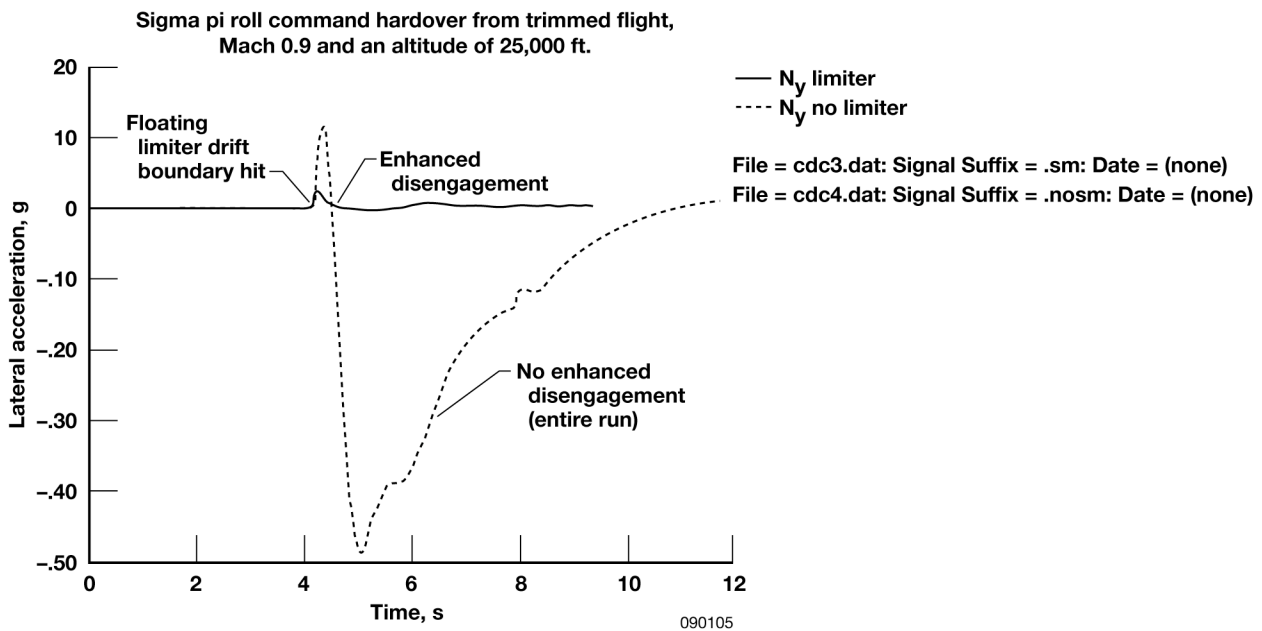


Figure 14. Lateral acceleration response due to an Airborne Research Test System roll hardover.

Floating Limiter

The floating limiter safety monitor (ref. 5) was required to allow full surface authority at the maximum actuator rates if required by the NN control laws while still protecting the pilot and aircraft from excessive forces in the case of a commanded hardover.

The floating limiter monitor automatically engages when the NN is activated, and works by computing the rate of change for each NN command and applying a moving upper and lower boundary limits window. The floating limiter structure is shown in figure 15. Full surface authority at the maximum actuator rates (within the moving window) is achieved, but with the limitation that the stick must be pulled back no faster than the drift rate of the floating limiter. This limiter and procedure still allow for normal piloted maneuvers such as wind-up turns, which is a reasonable compromise. The window constantly tries to center about the NN command rate, but is programmed to move at a much slower drift than is possible from NN command rates. This algorithm provides the desired protection from a commanded hardover. The NN command rates within the window boundaries are allowed to change at maximum rates since the commands are not in any one direction long enough to cause problems. If the NN command does persist in one direction, however, it will “catch up” with the floating limiter boundary and will be temporarily rate-limited to that value. When rate-limiting occurs, a persistence counter starts and a signal is sent to the NN control laws to stop learning. When the limit is reached for the persistence counter, a downmode command is generated. A maximum and minimum range limiter that would cause a disengage was also included.

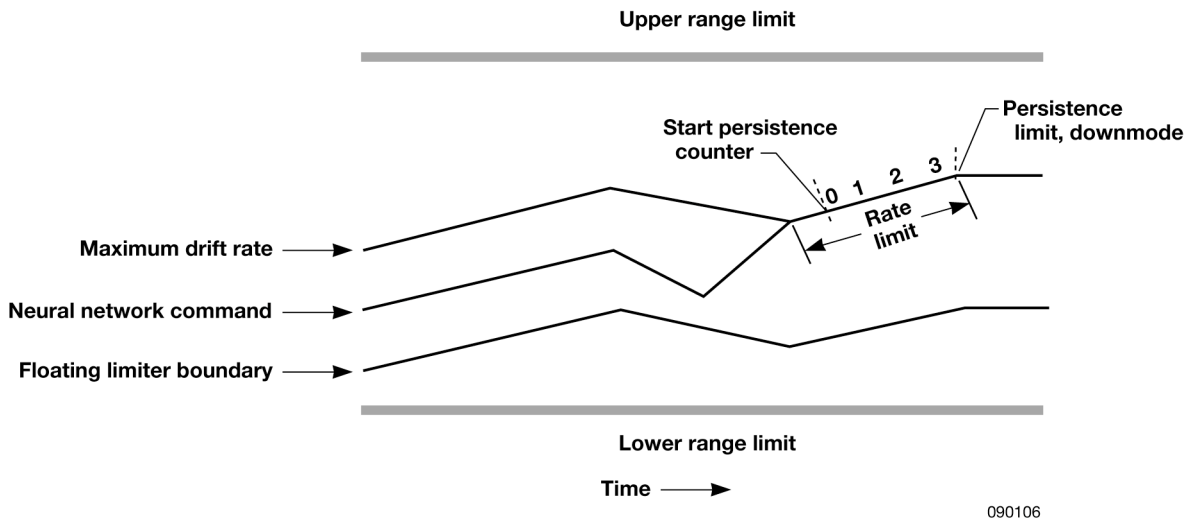


Figure 15. The floating limiter structure.

One of the problems in implementing the floating limiter was the desire to make the monitor very tight when the NN is initially engaged but no failures have been induced (a very small NN command), then open the limits after the failure is in a transition phase, and finally change the limits again after the failure has stabilized so the NN is allowed to generate the necessary commands to compensate for the failure without causing a downmode. This was solved by developing three floating limiter regions, as shown in figure 16. The set of constants used for the floating limiter is shown in table 4. These parameters were tuned using the DFRC simulator to meet the $\pm 0.5 g$ lateral, $+2 g$ normal accelerations, $< 80\%$ design limit load (DLL) requirements. Drift rates are independently set according to the axis, failure type, and magnitude. The drift, persistence, downmode, and range flags were added to a 1553 message from the FCC to the ARTS; these signals were also available on the instrumentation system for monitoring in the MCC.

Table 4. Floating limiter constants metrics.

Right stabilator failure from trim fl_drift_table_conf_file[][][]	P axis	Q axis	R axis
0 deg and no fail, dps ³ transition final	150 500	50 90	0.03 0.01
+2 deg, dps ³ transition final	230 700	60 60	0.03 0.02
+ 4 deg, dps ³ transition final	430 850	60 60	0.03 0.09
-2 deg, dps ³ transition final	230 525	60 60	0.03 0.02
-4 deg, dps ³ transition final	430 550	60 60	0.03 0.09
Canard angle of attack fails			
Set 1, dps ³ transition final	100 100	1 1	0.03 0.03
Set 2, dps ³ transition final	100 100	20 20	0.03 0.03
Metrics			
Initial drift, dps ³ fl_init_drift_conf_file[]	1.0	1.0	0.01
Delta, dps ² fl_delta_conf_file[]	200	52	0.10
Range limit, dps ² fl_hard_range_conf_file[]	775	300	0.2
Persistence time, s fl_persistence_time_conf_file[]	0.25	0.10	0.25
Transition time, s fl_transition_time_conf_file	3		

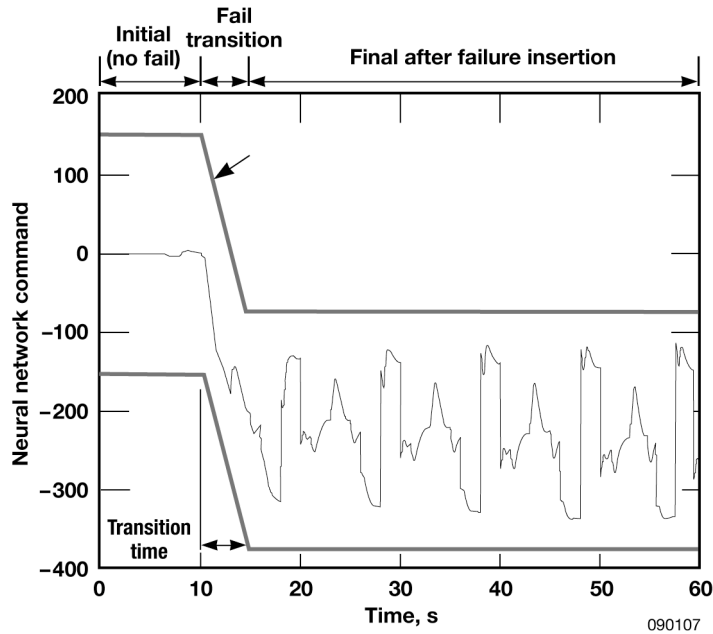


Figure 16. The floating limiter regions.

LOADS MODEL

The adaptive control algorithms were tested against the allowable load envelope of the IFCS airplane by running batch simulations of the loads clearance maneuvers with the analytical loads model in the loop (1 g half-stick 360° rolls, 4 g wind-up turns, and 3 g loaded roll reversals). These tests caused the floating limiter to detect an excessive rate of change in the NN commands, which resulted in a disengagement and return to the baseline conventional control laws, in each case hopefully before the loads exceeded 80% design limit load (DLL). Each batch simulation run consisted of selecting a loads clearance maneuver and inserting the hardover command at one time frame in the simulation; this was repeated at successive 0.5-s intervals for the duration of the maneuver. Thus, a 20-s maneuver generated 40 ARTS hardover runs. Any test conditions that showed a simulated ARTS failure to generate over 80% DLL on any of the load stations were not flown unless further analysis indicated that the pre-programmed stick inputs were partially responsible for high accelerations or surface positions. In these cases, additional runs were conducted using recorded pilot inputs to drive the batch simulation. If these runs showed less than or equal to 80% DLL, the suspect test conditions were flown. It should also be noted that in a few cases the floating limiter was too efficient, and would downmode within a few time frames of engagement or during the maneuver. This was typically due to exceeding the pitch rate floating limiter, and occurred on the largest stabilator-lock and canard multiplier cases. These difficulties were overcome by using pre-recorded pilot input files to drive the batch simulation; the human pilot was able to compensate for the reduced stability at the higher canard multipliers and the pilot-induced oscillation (PIO) tendency with the largest stabilator-lock. The 80% DLL cutoff was selected to give the airframe extra margin to compensate for uncertainty in the loads model and the adaptive controller algorithm.

The floating limiter algorithm prevents ARTS hardover commands from propagating to the FCC, thus preventing catastrophic load levels from high-rate hardover surface commands and accelerations. This is illustrated in figures 17 through 20. Figure 17 shows the N_z and N_y response due to a nominal 1 g trim condition with a canard failure multiplier of -0.5 inserted at 5 s and a hardover inserted at 15 s. With the floating limiter engaged, the peak N_z was approximately 2.5 g and the peak N_y was smaller than -0.25 g.

Without the floating limiter engaged, the N_z peaks at 11 g and the N_y peaks at -2.5 g. Figure 18 shows the loads predicted for forward fuselage station FS400. With the floating limiter engaged, the loads are well below the 80% DLL limit. Without the floating limiter engaged, the loads build to over 200% DLL for both vertical shear and the vertical-bending-to-lateral-bending strength envelope. Figures 17 and 18 show a nominal 1 g trim condition with a left stabilator lock at trim deflection inserted at -0.5 s and a hardover inserted at 15 s; figure 19 shows the N_z and N_y response. With the floating limiter engaged, the peak N_z was approximately 2.5 g and the peak N_y was smaller than -0.25 g. Without the floating limiter engaged, the N_z peaks at 8.5 g and the N_y peaks at -1.75 g. Figure 20 shows the loads predicted for forward fuselage station FS400. With the floating limiter engaged, the loads are well below the 80% DLL limit. Without the floating limiter engaged, the loads build to over -150% DLL for vertical shear, and the vertical-bending-to-lateral-bending strength envelope peaked at almost -125% DLL.

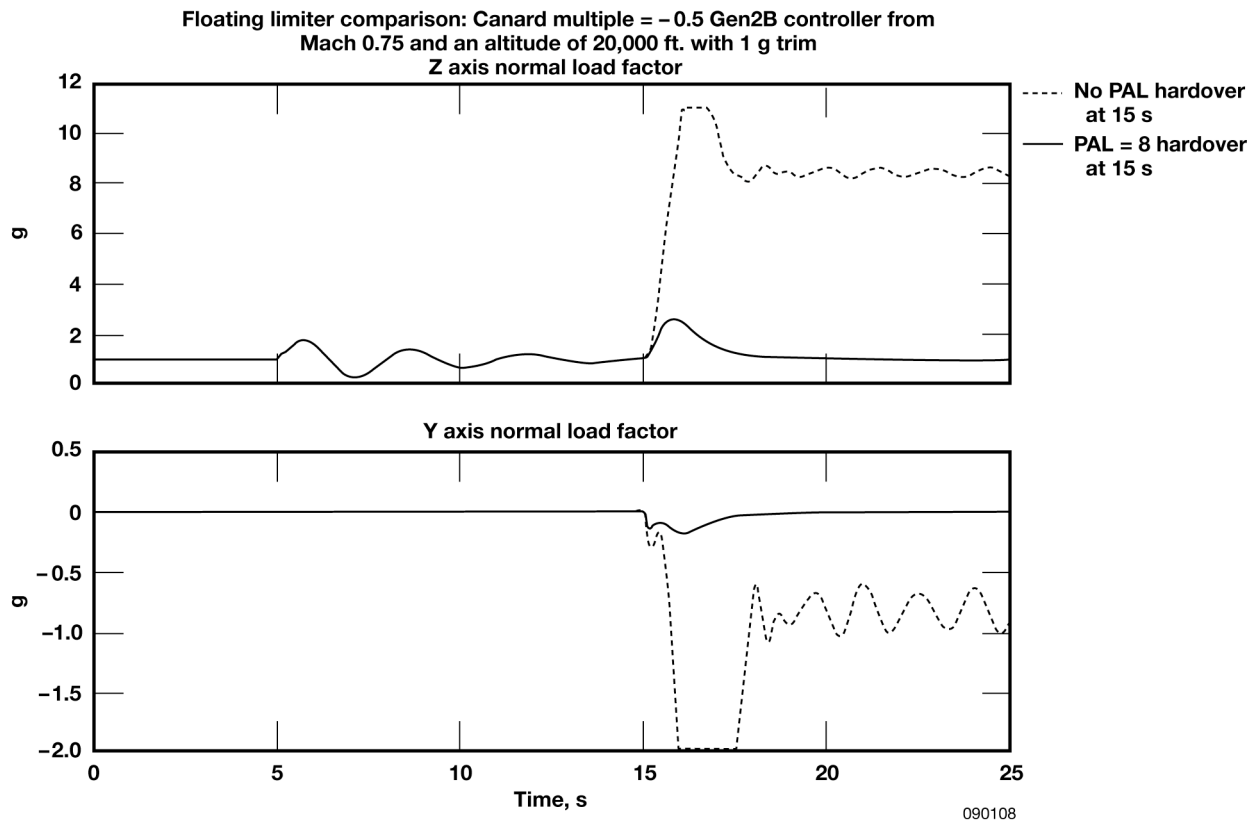


Figure 17. Simulated normal acceleration response, 1 g trim, canard multiplier of -0.5, with Airborne Research Test System hardover inserted at 15 s (PAL = 8, DAG = 28, CAT = 51).

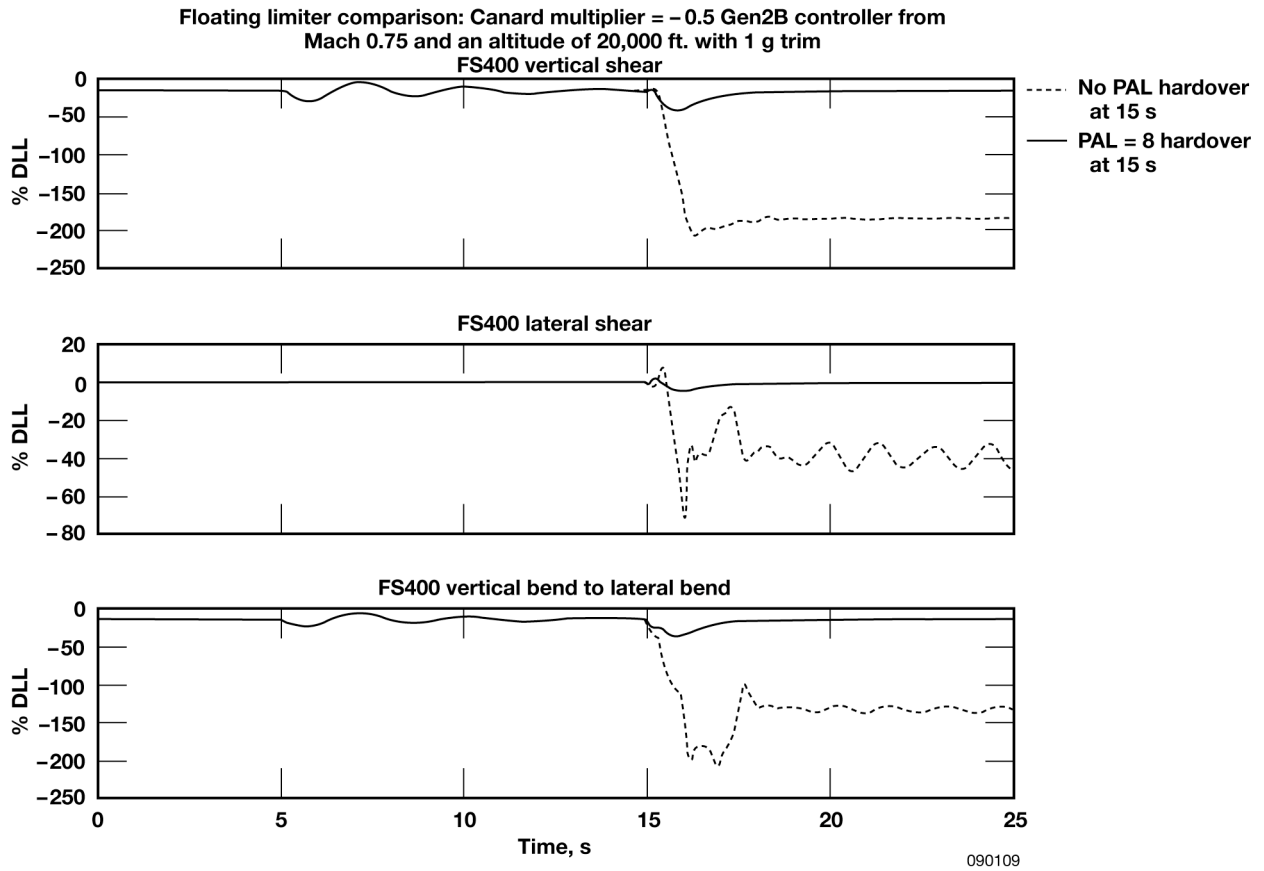


Figure 18. Simulated forward fuselage loads, 1 g trim, canard multiplier of -0.5, with Airborne Research Test System hardover inserted at 15 s (PAL = 8, DAG = 28, CAT = 5 1).

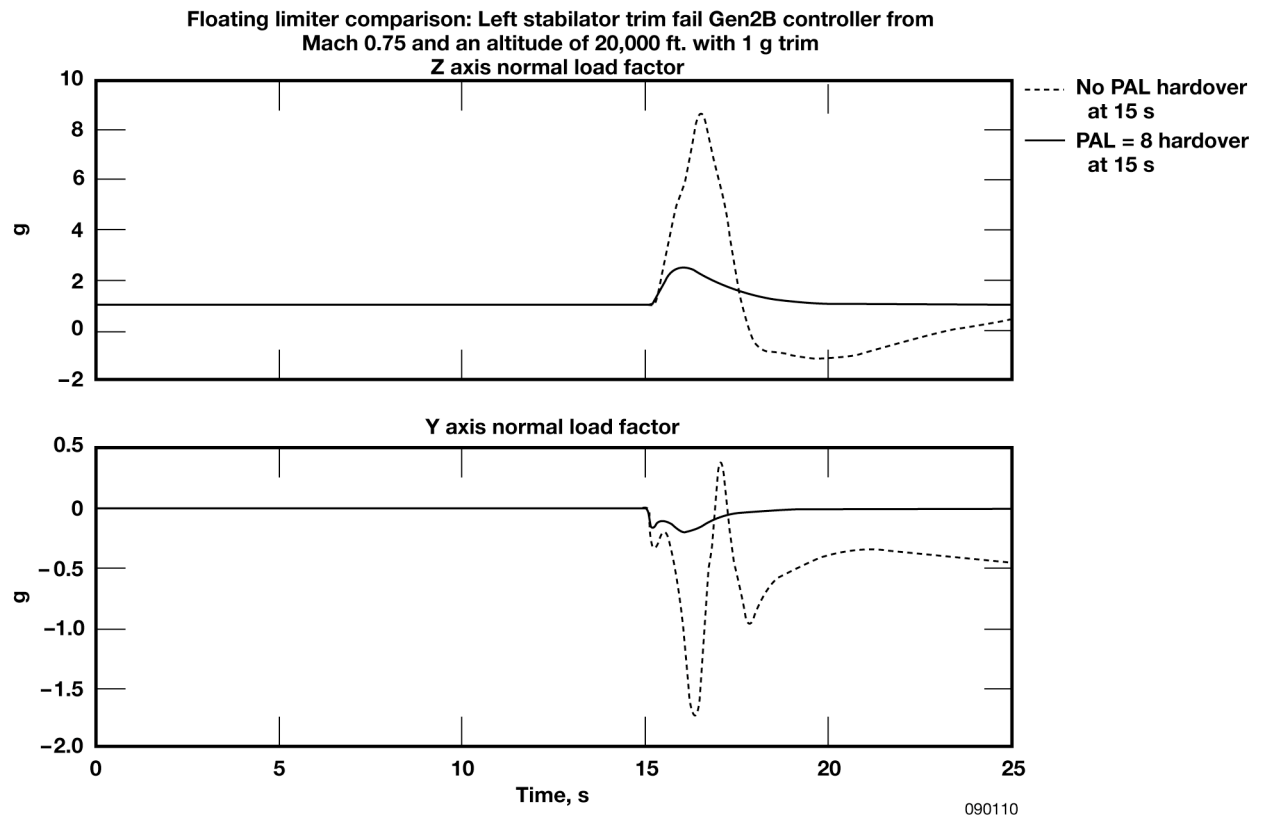


Figure 19. Simulated normal acceleration response, 1 g trim, left stabilator locked at trim deflection, with Airborne Research Test System hardover inserted at 15 s (PAL = 8, DAG = 23, CAT = 51).

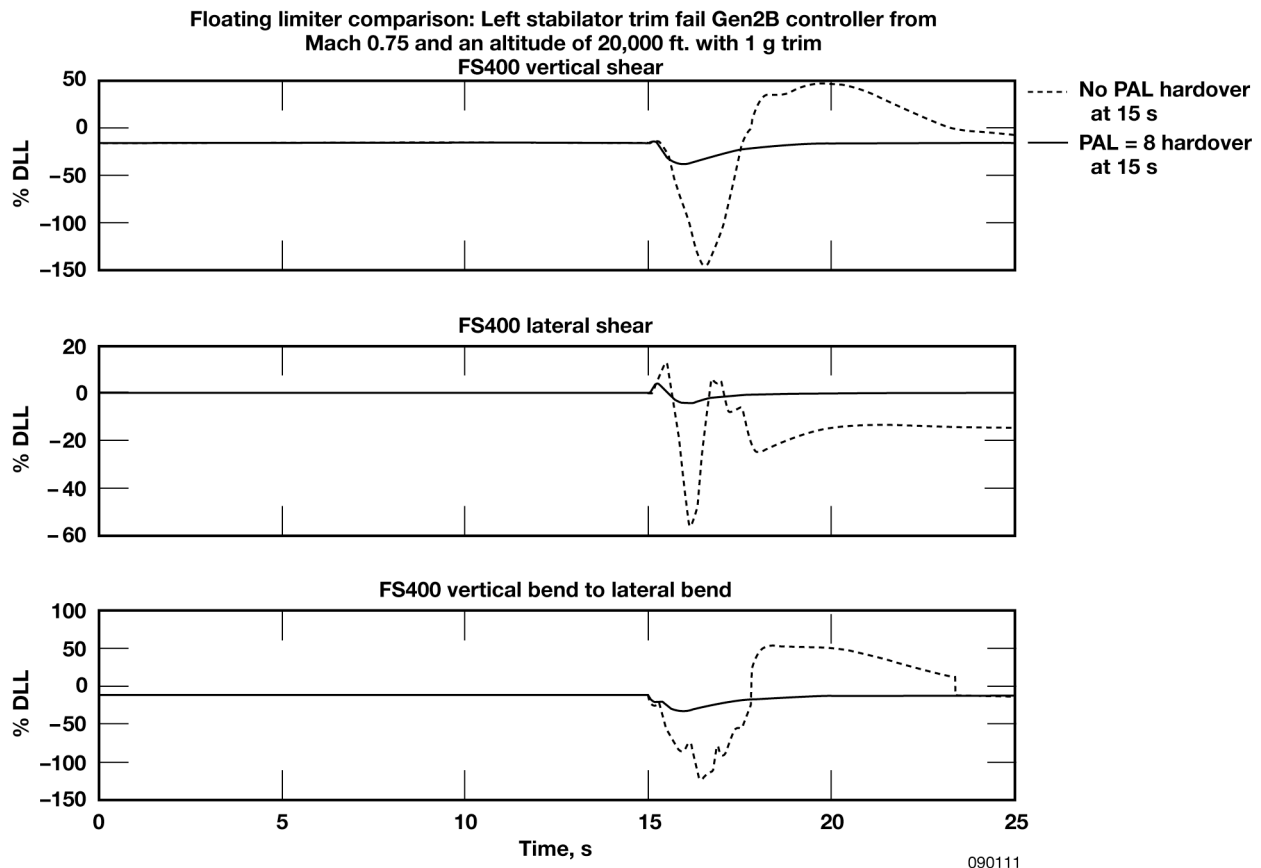
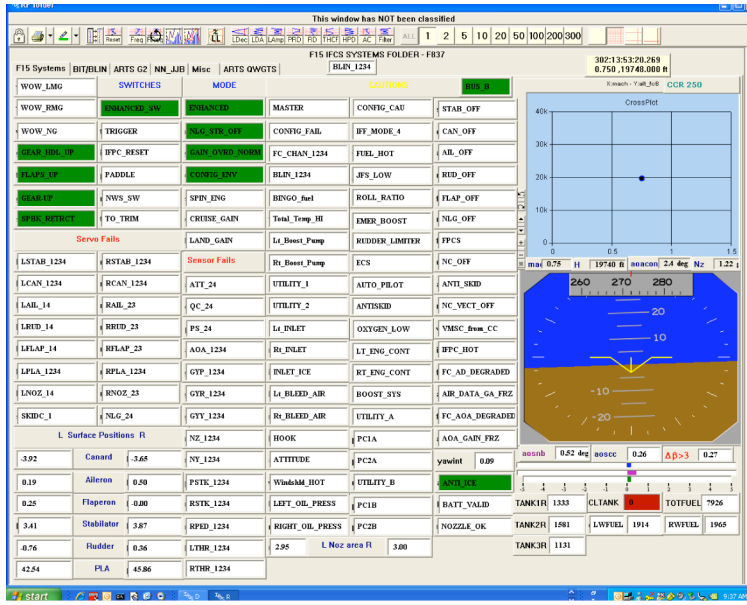


Figure 20. Simulated forward fuselage loads, 1 g trim, left stabilator locked at trim deflection, with Airborne Research Test System hardover inserted at 15 s (PAL = 8, DAG = 23, CAT = 51).

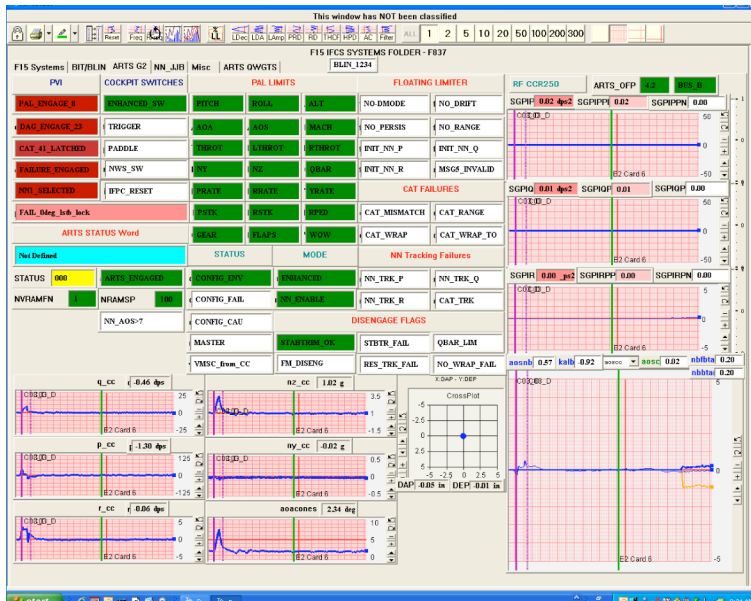
INTERACTIVE ANALYSIS AND DISPLAY SYSTEM DISPLAYS

The NASA DFRC team replaced the MCC computers with PCs to enable utilization of the Symionics (Arcadia, California) real-time display system called the Interactive Analysis and Display System (IADS). Three of the MCC displays developed by the systems engineers are shown in figures 21, 22, and 23. The basic F-15 systems display page is shown in figure 21. Signals such as aircraft health, mode, configuration, surface positions, and fuel quantities are shown. Failures were programmed to display in red. The IADS design environment enables quick prototyping of display pages including derived parameters using C-type expressions. For example, when a BLIN code is set, the display is programmed to blink to capture the attention of the systems engineer so that another page may be selected for viewing a code description. The primary NN display page is shown in figure 22. This page displays the selected PVI parameters (PAL, DAG, and CAT). If a PAL limit has been exceeded, that limit will display in red and will “latch” until the pilot cycles the mode switch in the cockpit. The NN weights display page is shown in figure 23. The weights for each axis are displayed in both strip chart and tabular form. Some of the components used to build an IADS display will now be discussed.



090112

Figure 21. The interactive analysis and display system: the basic F-15 systems display page.



090113

Figure 22. The interactive analysis and display system: neural network systems page 1.

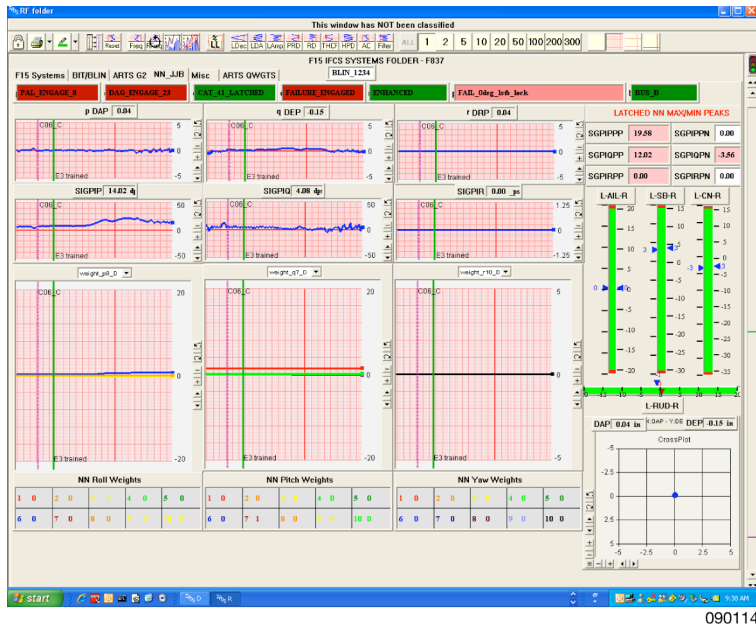


Figure 23. The interactive analysis and display system: neural network systems page 2.

Alphanumeric Widgets

The alphanumeric widget display types were used in great number because they enabled easy creation of derived parameters and permitted multiple test strings to be displayed depending on the value of that signal. String colors were added, corresponding to different signal values. The alphanumeric widget data structure enabled the display and processing of a large amount of information.

Strip Charts

Multiple parameters displaying assigned colors were also used in a single strip chart so that if a particular test event was missed, the scroll bar on the far right could be used to go back in time to view the event.

Slider Bars

A slider bar was also implemented, to assist with visualization of the control surface motion in relation to the other surfaces. The slider bar is shown in figure 24.

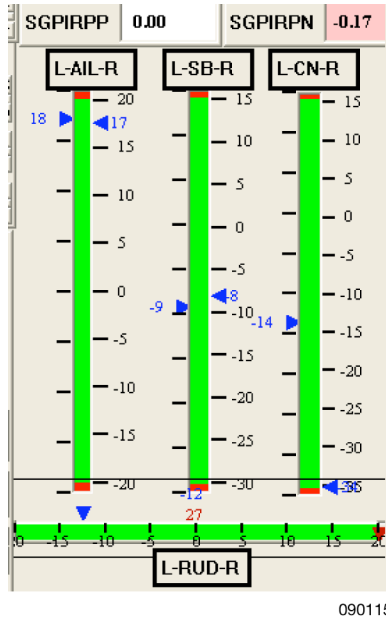


Figure 24. The slider bar display.

Latched Functions

The latched functions feature was created as a derived parameter. For example, peak maximum and minimum NN commands were programmed in IADS to show the limit excursions. Latching reset logic was also performed in the IADS configuration files.

Flasher Functions

Flasher functions were used on the IADS display to enhance human awareness of any serious problem that required immediate response. The flashers were used for an F-15 BLIN code situation, and to indicate if the display pages were not receiving new data.

Built-in Displays

One of the built-in IADS displays for the attitude displacement indicator (ADI) is shown in figure 25. This display provided situational awareness to the control room of the airplane attitude.

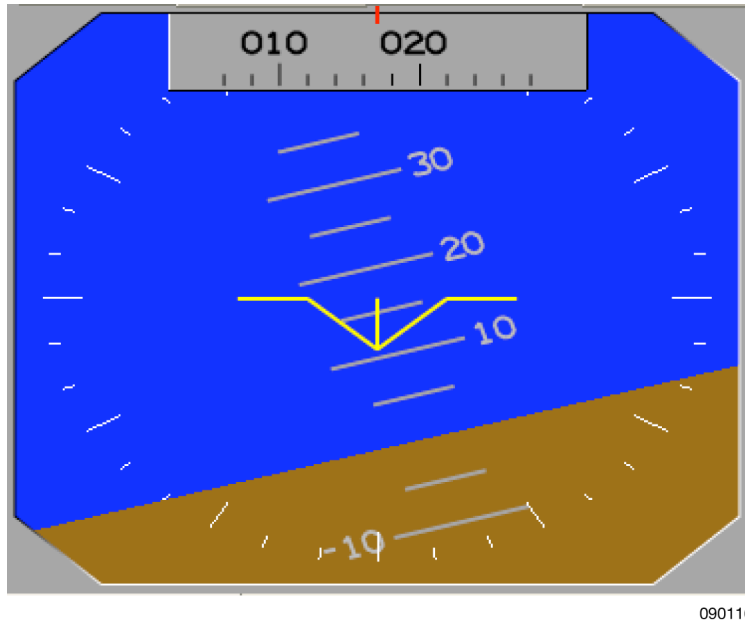
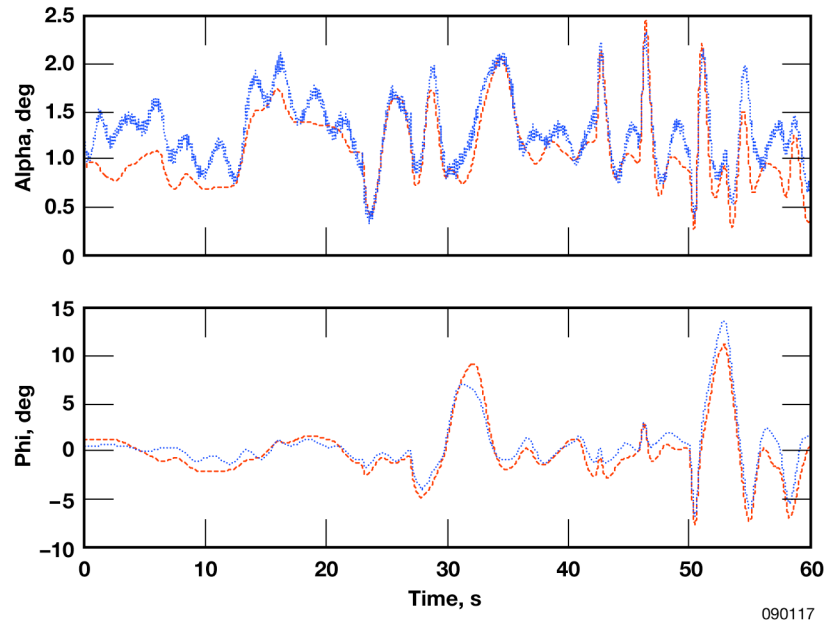


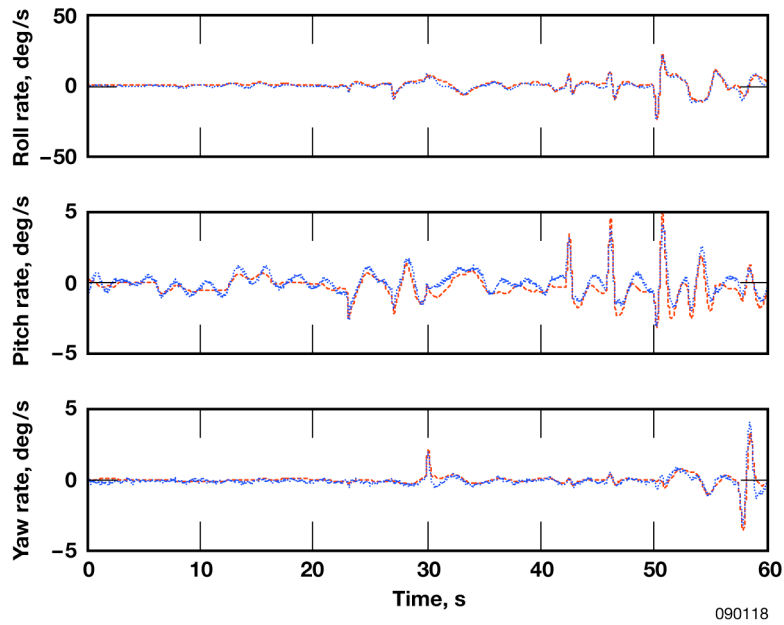
Figure 25. The attitude displacement indicator display.

FLIGHT-TEST RESULTS

This section discusses the comparison of the flight-test results and the simulation. The stick and rudder positions from flight were recorded and used as inputs to drive the simulation. The flight-test results are from the Gen 2a adaptive controller with a left stabilator failed at trim 7.5 s into the maneuver. The flight conditions were Mach .75 at an altitude of 20,000 ft. The flight response data (pitch and roll stick, rudder pedals, and throttle commands) were recorded from flight and back-driven into the simulation to see how closely the responses would match. Figure 26(a) shows the angle of attack (α) and bank angle (ϕ) from the flight (blue) and the simulation (red). Figure 26(b) shows the flight (blue) roll rate, p , pitch rate, q , and the yaw rate, r , and the simulation (red) p , q , and r . Neural network outputs, which are the roll axis signal, the pitch axis signal, and the yaw axis signal, are shown in figure 26(c): flight data is displayed in blue, and simulation results in red.

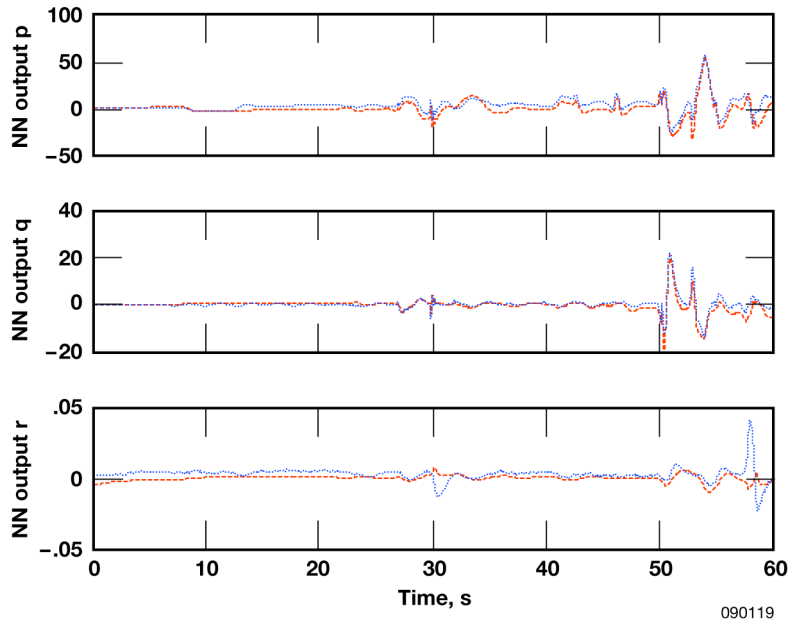


(a). Flight (blue lines) to simulation (red lines) comparison of alpha and phi for left; the stabilator jammed at 7.5 s.



(b). Flight (blue lines) to simulation (red lines) comparison of p, q, and r for left; the stabilator jammed at 7.5 s.

Figure 26. Comparisons of flight to simulation.



(c). Flight (blue lines) to simulation (red lines) comparison of the neural network signals for left; the stabilator jammed at 7.5 s.

Figure 26. Concluded.

The flight-to-simulation comparison time histories match very well. The results show that the simulation did a very good job of predicting the behavior of the actual aircraft response. The only exception is the yaw axis NN signal shown in figure 26(c); however, upon closer examination of this signal the size or magnitude of the yaw axis signal can be observed to be very small. The yaw axis response is very difficult to match even in a healthy airplane.

CONCLUSION

A safe, cost-effective approach was undertaken by the NASA Dryden Flight Research Center (Edwards, California) to investigate experimental adaptive control algorithms. This approach utilized a simplified, single-string Airborne Research Test System that interfaced with the existing flight control computers of the McDonnell-Douglas NF-15B airplane. The pilot-vehicle interface design allowed for flexibility of various options during the flight tests. All Generation 2a software was verified and validated using the Dryden F-15 simulation. The pilot-vehicle interface design also allowed for considerable flexibility in selecting such neural network algorithms, failure combinations, and excitations systems as were required for flight test.

The verification and validation of the neural network software was thorough and efficient. Some of the problems that were identified were corrected with new configuration files not requiring a new compile of the operational flight program. Certain DRs were considered minor and were not fixed; these were handled using procedures to work around the problem.

Safety was the primary consideration in preparing for flight test. Any problem with the neural network would result in a downmode back to the conventional flight control computer control laws. The worst case scenario that was considered was if the neural network commands were to go hard over (command a rapid and sustained displacement of an aircraft aerodynamic control surface). A floating

limiter was designed to protect the structure forces of the airplane and to meet the pilot-imposed maximum g excursions. A loads model in the Dryden simulator was used extensively to validate the floating limiter disengage metrics.

Interactive analysis and display system display pages, developed by the flight-test engineers for monitoring in the Mission Control Center, proved to be easy to build and very effective. The derived functions capability within the interactive analysis and display system helped immensely to convert raw signal constructs into user-friendly formats that provided insight to both the neural network and the basic F-15 airplane systems.

REFERENCES

1. Calise, A. J., S. Lee, and M. Sharma, "Direct Adaptive Reconfigurable Control of a Tailless Fighter Aircraft," AIAA-98-4108, 1998.
2. Rysdyk, Rolf T., and Anthony J. Calise, "Fault Tolerant Flight Control Via Adaptive Neural Network Augmentation," AIAA-98-4483, 1998.
3. U.S. Department of Defense, "Flying Qualities of Piloted Vehicles," MIL-STD-1797, 1987.
4. Kaneshige, John, and John Burken, "Enhancements to a Neural Adaptive Flight Control System for a Modified F-15 Aircraft," AIAA-2008-6986, 2008.
5. Perhinschi, Mario G., Marcello R. Napolitano, Giampiero Campa, Brad Seanor, John Burken, and Richard Larson, "Design of Safety Monitor Schemes for a Fault Tolerant Flight Control System," *IEEE Transactions on Aerospace and Electronic Systems*, Vol. 42, No. 2, p. 562.

REPORT DOCUMENTATION PAGE				Form Approved OMB No. 0704-0188	
<p>The public reporting burden for this collection of information is estimated to average 1 hour per response, including the time for reviewing instructions, searching existing data sources, gathering and maintaining the data needed, and completing and reviewing the collection of information. Send comments regarding this burden estimate or any other aspect of this collection of information, including suggestions for reducing this burden, to Department of Defense, Washington Headquarters Services, Directorate for Information Operations and Reports (0704-0188), 1215 Jefferson Davis Highway, Suite 1204, Arlington, VA 22202-4302. Respondents should be aware that notwithstanding any other provision of law, no person shall be subject to any penalty for failing to comply with a collection of information if it does not display a currently valid OMB control number.</p> <p>PLEASE DO NOT RETURN YOUR FORM TO THE ABOVE ADDRESS.</p>					
1. REPORT DATE (DD-MM-YYYY) 01-07-2009		2. REPORT TYPE Technical Memorandum		3. DATES COVERED (From - To)	
4. TITLE AND SUBTITLE Implementation of an Adaptive Controller System from Concept to Flight Test				5a. CONTRACT NUMBER	
				5b. GRANT NUMBER	
				5c. PROGRAM ELEMENT NUMBER	
6. AUTHOR(S) Ricahrd R. Larson, John J. Burken, Bradley S. Butler, and Steve Yokum				5d. PROJECT NUMBER	
				5e. TASK NUMBER	
				5f. WORK UNIT NUMBER	
7. PERFORMING ORGANIZATION NAME(S) AND ADDRESS(ES) NASA Dryden Flight Research Center P.O. Box 273 Edwards, California 93523-0273				8. PERFORMING ORGANIZATION REPORT NUMBER H-2973	
9. SPONSORING/MONITORING AGENCY NAME(S) AND ADDRESS(ES) National Aeronautics and Space Administration Washington, DC 20546-001				10. SPONSORING/MONITOR'S ACRONYM(S) NASA	
				11. SPONSORING/MONITORING REPORT NUMBER NASA/TM-2009-214648	
12. DISTRIBUTION/AVAILABILITY STATEMENT Unclassified -- Unlimited Subject Category 05 Availability: NASA CASI (301) 621-0390 Distribution: Standard					
13. SUPPLEMENTARY NOTES Larson, Burken, and Butler, NASA Dryden Flight Research Center; Yokum, West Virginia High Technology Consortium Foundation. Also presented as AIAA-2009-2055 at the AIAA Infotech@Aerospace Conference and Exhibit, Seattle, Washington, April 6-9, 2009.					
14. ABSTRACT The National Aeronautics and Space Administration Dryden Flight Research Center (Edwards, California) is conducting ongoing flight research using adaptive controller algorithms. A highly modified McDonnell-Douglas NF-15B airplane called the F-15 Intelligent Flight Control System (IFCS) is used to test and develop these algorithms. Modifications to this airplane include adding canards and changing the flight control systems to interface a single-string research controller processor for neural network algorithms. Research goals include demonstration of revolutionary control approaches that can efficiently optimize aircraft performance in both normal and failure conditions and advancement of neural-network-based flight control technology for new aerospace system designs. This report presents an overview of the processes utilized to develop adaptive controller algorithms during a flight-test program, including a description of initial adaptive controller concepts and a discussion of modeling formulation and performance testing. Design finalization led to integration with the system interfaces, verification of the software, validation of the hardware to the requirements, design of failure detection, development of safety limiters to minimize the effect of erroneous neural network commands, and creation of flight test control room displays to maximize human situational awareness; these are also discussed.					
15. SUBJECT TERMS Adaptive controllers, F-15, IFCS, Safety monitors, Verification and validation					
16. SECURITY CLASSIFICATION OF:			17. LIMITATION OF ABSTRACT	18. NUMBER OF PAGES	19b. NAME OF RESPONSIBLE PERSON
a. REPORT	b. ABSTRACT	c. THIS PAGE			STI Help Desk (443) 757-5802
U	U	U	UU	39	19b. TELEPHONE NUMBER (Include area code) (443) 757-5802